UNIVERSITY OF NAIROBI

Assessing the Hydrocarbon Potential of Offshore Lamu Basin using Nuclear Well Logs

By

Simiyu Wanjala Cleophas, BSc (Geology)

A thesis submitted in partial fulfillment of the requirement for the award of degree of Master of Science in Nuclear Science at the University of Nairobi

Declaration

This thesis is my original work and has not been submitted for examination and award of any degree at any other University or institution of higher learning. Where other people`s work has been used, it has been acknowledged and referenced in accordance with the University of Nairobi requirements.

Simiyu Wanjala, Cleophas, S56/61781/2013
Institute of Nuclear Science and Technology, University of Nairobi.

Signature ……. Date…….

Supervisors' Approval

This thesis has been submitted for examination with our knowledge as university supervisors:

1) Mr. Michael J. Mangala
   Institute of Nuclear Science and Technology
   University of Nairobi

   Signature…… Date…….

2) Prof. Jayanti P. Patel
   Department of Physics
   University of Nairobi

   Signature…… Date…….

Dedication

To my late father, Maina Wanjala Maelo

To my extended family back home that may never know what am doing

Acknowledgement

My appreciation goes to the data custodian-National Oil Corporation of Kenya and particularly the General Manager-Upstream, Dr. Kivuti Nyagah for granting me access and use of well log data for this project. I would also like to thank my supervisors; Mr. Michael J. Mangala for his invaluable guidance throughout the project work, and Prof. Jayanti P. Patel for his critical and thoughtful suggestions during this research.

Finally, to my wife Faith and the kids; thanks for your patience, understanding, and support at all times.

Abstract

Kenya's sedimentary basins are similar to other basins in eastern Africa where petroleum has been discovered. In general, acoustic and electrical methods are used in geophysical logging for hydrocarbon exploration in the country. However, the recent discovery of oil in Turkana, a region initially dismissed as non-viable has prompted review of previous data and integration of modern nuclear logging techniques in exploration. The core objective of this study was to use nuclear well log data to assess the hydrocarbon potential in Offshore Lamu basin. The neutron log, density log, and gamma log data for Simba-1, Kofia-1 and Maridadi-1B wells were acquired from National Oil Corporation of Kenya. The log data in LAS format were subjected to well log analysis, interpretation, and presentation techniques using notepad++, ArcGIS, and Techlog software. The results were integrated with electric log data and cuttings reports whenever available for quality control and data validation. Essentially, the study determined petrophysical parameters mainly: lithology, volume of shale (V_{sh}), porosity, and fluid saturation to gauge the hydrocarbon reservoir characteristics of the basin. The results show, on average, three zones of interest in study area, range between 2600 m-3900 m below mean sea level. Sandstones and limestones are the predicted reservoir formations, while shale is the interpreted source rock. The porosity at the zones of interest in the three wells is placed at 21% - 35%, although there are lower values for regions viewed as tight carbonate reservoir zones. The V_{sh} is lower, estimated at 16% - 24% in projected reservoir zones, with high resistivity, probably due to presence of hydrocarbons. Predicted water saturation is high (30% - 60%) and exceed the recommended 30% average. This has been attributed to bound water in regions where V_{sh} is high, or low hydrocarbon content in clean sandstones. Estimated permeability mainly derived from porosity values ranges from 21 mD to 116 mD in single oil reservoir layers. The results for porosity and permeability, and V_{sh} are within the values of most oilfield discoveries. There is presence of hydrocarbons in the Lamu basin but whose quantity is undeterminable. In conclusion, the study recommends drilling of directional wells, and the use of seismic and NMR data as a determinant of bound fluids in complex lithology.

Key words: nuclear logs, porosity, saturation, permeability, volume of shale

Table of Contents

List of Tables

List of Figures

List of Abbreviations

API–American Petroleum Institute

ASCII–American Standard Code for Information Interchange

bbl – barrel (5.6154 cu.ft or 0.159 m^3, equivalent to 159 litres)

CNL – Compensated Neutron Log

DST – Drill Stem Test

GR–Gamma Ray reading

HC–Hydrocarbons (crude oil and natural gas)

HI – Hydrogen index

IOC–International Oil Company

KCl–Potassium chloride polymer drilling mud-used to inhibit clay hydration (shale stabilizer)

LAS–Log ASCII Standard (common file-format for storing wellbore log data in HC exploration)

LLD–Deep Laterolog

LLS–Shallow Laterolog

NMR – Nuclear Magnetic Resonance

NOCK – National Oil Corporation of Kenya

RHOB–Bulk Density

$\mathbf{R_w}$ – Resistivity of formation water

SCF – standard cubic feet

SP–Spontaneous Potential

$\mathbf{S_w}$ – Water saturation

TCR – Total Core Recovery

TOC – Total Organic Carbon

$\mathbf{V_{sh}}$ – Volume of Shale

CHAPTER ONE: INTRODUCTION

1.1 Background

While more than half of Kenya's sedimentary basins are considered geologically akin to other eastern Africa regions where hydrocarbons (HCs) have been discovered. Intensive exploration activities by numerous International Oil Companies (IOCs) since the 1950's had not yielded any economical reserves till the year 2012. Nevertheless, large discoveries in Mozambique, Tanzania, Ethiopia, Sudan, and the heavy HC deposits on the conjugate Madagascar margin indicate hydrocarbon potential in East Africa (Osicki et al., 2015). Still, most prospecting companies abandoned their exploration activities in Kenya having incurred heavy losses without making any discovery. This trend changed in the year 2012 when Tullow Oil declared commercially viable crude oil find in the Tertiary rift basin.

The discovery of oil in an area that had earlier been dismissed as non-viable has been attributed partly to review of previous data and advancement in exploration techniques, particularly, well logging (Zongying et al., 2013). Well logging is a term that implies recording of information in relation to depth or time. Krygowski and Asquith (2005) state that a well log is aimed at acquiring information through measurement of several chemical, lithological and physical nature of geological material. This data when complemented with others from core examination endeavors to provide details on nature of formation, depth, porosity, permeability, and fluid type among other specifics. Furthermore, the need for precision in well-logging has been achieved by the advent of computers and advancement in instrumentation and electronics that has enabled recording of huge amount of data in real time in Log ASCII Standard (LAS) format (Doveton, 1994).

Nuclear well logging has played a significant role in the past 50 years in the discovery and exploitation of hydrocarbons. Drilling by itself does not deliver explicit facts about the formations. Rock cuttings may provide information on the lithology present but are not clear on the exact depth and thickness. Even coring, that is normally prohibitively expensive gives inadequate data on formation fluids, in addition to the fact that Total Core Recovery (TCR)

rarely gets to 100 percent. Therefore, there is need for a range of well logs to be assembled in order to guarantee exhaustive formation evaluation (Harvey and Lovell, 1998). Furthermore, Heart et al. (2000), claims that precise determination of petrophysical parameters is necessary to characterize the commercial viability for the development of hydrocarbon reservoirs.

In the developed world, the industry support companies such as Schlumberger, Baker Hughes and Halliburton have varied advanced logging systems (Doveton, 1994), whose developments have found applications in hydrocarbon as well as other mineral exploration and ground water investigations in Kenya. An effort is herein made to illustrate the application of nuclear well logging in oil and gas exploration in Kenya.

1.2 Statement of the Problem

The demand for adequate and reliable energy sources is key in Kenya's quest to transit into a Newly Industrialized Economy by the year 2030 through manufacturing. To insure successful offshore exploration activities requires accurate determination of petrophysical parameters. This is because the quantity of hydrocarbon in a prospective reservoir is mainly a product of the HC saturation and its porosity. Besides the HC saturation and porosity, there is need to know the rock volume containing oil and gas so as to approximate total reserves and to establish the economic viability of the accumulation (Ellis, 1987).

The volume of HCs in the reservoir can be computed with the knowledge from its area and thickness, and from other parameters deduced from well log data. The input of petrophysical parameters is important in the decision making concerning the economic viability of a hydrocarbon prospect.

1.3 Research Objectives

1.3.1 Broad Objective

This study focused on the petrophysical data estimations and analysis for characterizing the hydrocarbon potential within the Lamu Basin. It demonstrates the application of nuclear technology in the petroleum exploration industry, particularly in resource characterization and reservoir analysis. The study was carried out in three selected wells with the succeeding detailed objectives.

1.3.2 Specific Objectives

i. To assess the response of nuclear logs and identify zones of interest in the wells, corresponding to; low GR, low bulk density, high resistivity, mud-cake formation;
ii. To determine petrophysical parameters at the zones of interest in the wellbore;
iii. To establish the presence and nature of hydrocarbons in the studied wells.

1.4 Justification of the study

Nyagah (1995) asserts that hydrocarbon shows have been reported in about ten wells drilled within the Lamu basin. Most of the gas shows and oil stains have been revealed in cretaceous and tertiary formations, mainly sandstone reservoirs. The results from these wells notwithstanding, exploration firms have deemed it fit to declare that the reservoir potential is not sufficiently economical to necessitate additional development (NOCK, 1995). It can be hypothesized, from the above findings that Lamu Basin has inadequate potential for hydrocarbons. Hence, the question "is Lamu basin HC deposits economically viable"?

The essential components for the existence of hydrocarbon bearing reservoir in Lamu Basin have been proved by seismic data acquisition and drilling of exploratory wells (Nyaga, 1995). The presence of shale and sandstone/limestone as source rock and reservoir quality rocks respectively, amid structural traps charged with the potential for hydrocarbons is evident. Nonetheless, due to the complexity of reservoir structures and the expenditure allied to an offshore resource development, it is not yet known whether this hydrocarbon resource can be developed.

However, with the use of contemporary well logging techniques with superior data acquisition, the need for nuclear log analysis for petrophyiscal parameters of reservoir wells cannot be underscored (Abouzaid et al., 2016). Consequently, this research has investigated the application and usefulness of nuclear well log techniques in-hydrocarbon exploration-to Kenya's energy sufficiency strategy for vision 2030. Currently, thermal power generation in the country relies on expensively imported oil and gas.

1.5 Scope and limitation the study

From the year 1956 several exploratory wells were drilled, approximately thirty (30) in Lamu basin but were abandoned because the discovered oil was not economically viable. The wells have been grouped based on data available and geographic location. In this study, representative wells; Kofia-1, Simba-1, and Maridadi-1B were chosen for a nuclear well log investigation and geophysical analysis for petrophysical parameter evaluation. The data were acquired from NOCK during the year 2016 to 2017.

Cross plots and curve trends from compensated neutron log, gamma (GR) log, and density log were used for formation evaluation and fluid detection. Other geophysical log data such as electrical, spontaneous potential (SP), and caliper were integrated where available for data validation.

CHAPTER TWO: LITERATURE REVIEW

2.1 Overview

While well logging can be considered to be a comparatively young science, preliminary work can be traced back to 1869. Crain (1986) states that by the time Drake made the earliest oil discovery in the United States, Lord Kelvin of the United Kingdom was interpreting heat flow in shallow boreholes through the measurement of temperature vs. depth. Historical reviews of well logging have been published by Allaud and Martin (1977) and Johnson (1962). In the 50th Anniversary Issue of Geophysics, there is a publication by Segesman (1980) on the historical review of well logs spanning over 50 years. Due to the broad nature of the subject matter, the scope of review is limited to nuclear well logging for petrophysical measurements (Archie, 1942).

Asquith (1985) suggests that a geophysical log is meant to give important information with reference to the physical and geological conditions in and around a wellbore. Essential well log interpretation has for years remained the same. Just about all hydrocarbons exploited today emanate from a buildup in the pore spaces of dolomites, sandstones, or limestones-reservoir rocks (Helander, 1983). In general, the necessary elements for commercial hydrocarbon accumulation include: mature source formation-usually shale, geological reservoir material-sandstone, migration pathway linking the source to the reservoir, and an impervious cap rock or seal overlying the reservoir rock. Tiab and Donaldson (2004) argue that ultimately, the source rock, reservoir rock and seal ought to be set in a manner that the hydrocarbon is trapped.

2.2 History of Well Logging

According to Crain (1986), it is E.G Leonardon and the Schlumberger brothers who first published a comprehensible technical manuscript on log interpretation in 1934, on the the use of electrical resistivity log. Ever since, immense advances have been accomplished to date in logging and acquisition techniques and interpretation of well log data (Baker-Hughes-Atlas, 2002). Earlier data in log analysis entailed recognition of curves visually determined from the logged data when plotted verses depth. The shape of curves was correlated to core description

and rock sample information. The correlation is then used to establish a universal rule of thumb for identifying porous, permeable, and HC-bearing bed zones (Schlumberger, 1987).

The first application of radioactive properties in well logging was when neutron tools and gamma ray (GR) were used. Unlike resistivity and spontaneous potential (SP) tools, the nuclear methods have the ability to log formations filled with gas or air as well as through steel casing. The neutron log was considered as an indicator of porosity at around 1950 (Gaymard and Poupon, 1968). Nevertheless, the initial neutron logs were seriously affected by the wellbore conditions.

Liu (2017) asserts that the neutron log was accepted as a porosity measurement only after the 1962 presentation of the sidewall neutron porosity, and subsequent introduction of the compensated neutron equipment in 1970. A combination of the two neutron measurements into a single tool is what is referred to as the Dual Porosity neutron tool (Johnson, 1962). Still, early attempts at determining porosity utilized micro resistivity measurements. Other logging tools comprise nuclear spectrometry, Nuclear Magnetic Resonance (NMR), and several cased hole utilities (Jackson, 2001).

To date, well logging is frequently conducted by means of digital information acquisition podia. The data saved in file format-mostly LAS format, may contain application of broad numerical computation. Intelligent software utilizes the same and every so often better procedure than how their human equivalents formerly performed. Doveton (1994) argues that these developments have resulted into a quicker and every so often "smarter" understanding. Confidence to interpretation is built by applying modifications to raw data and carrying out 'sanity' checks on outcomes among other steps. This novel approach was employed to enable characterize the hydrocarbon potential of offshore Lamu basin (Nyaga, 1995).

2.3 Geology of the Lamu Basin

The Lamu Basin is the largest sedimentary basin in Kenya covering over 260,000 km^2 that occupy south-east Kenya (Figure 2.1). According to Zongying et al (2013), the basin boasts more than 10,000 m of sediments that contain possible source rocks and reservoir formations. Petroleum exploration in the basin is limited, to barely 30 wells, twenty (20) of which are associated with HC shows. Osicki et al. (2015) reports that, of the 8 offshore wells drilled, Sunbird-1's Miocene reefs revealed a few meters of gross oil column in 2014, and considerable depth of net gas pay encountered by Mbawa-1 in turbidities and channel sands in 2012.

An updated well location map including the recent discoveries in the tertiary rift where nuclear logging technique was successfully applied is presented in Appendix A1.

Lamu Basin is part of a failed Cretaceous-Tertiary rift with good analogies to India's Cambay and Bombay basins. Studies show that Lamu basin is bound by faults and it formed as a consequence of rifting during the Paleozoic-Mesozoic time that occurred on the start of Gondwana disintegration (Kerr et al., 1996).

The subsequent graben was jam-packed with continental Karroo siliciclastic (Permian-Jurassic) sediments. Carbonate formations related to the invasion of the Tethyan Sea are dominant in the basin deposits of the Jurassic time as shown in appendix A2 after Zongying et al. (2013).

The end of relative movement between Africa and Madagascar in the Cretaceous signaled the development of passive margin and progradation of deltaic deposits till the Paleogene (Nyagah, 1995). Low water bodies transgressed this basin during Miocene when one more carbonate system was dominant.

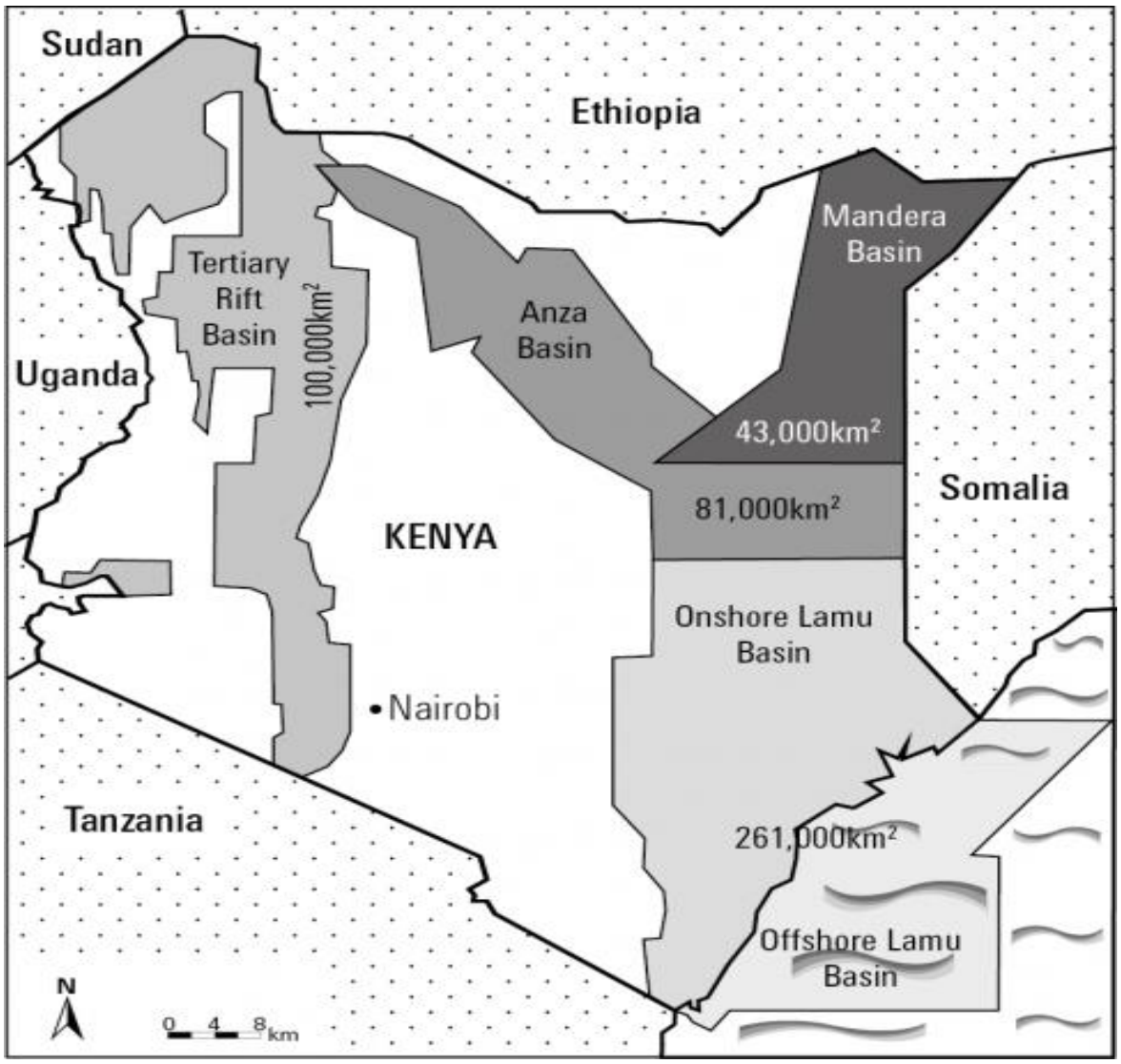

Figure 2.1: Location of Lamu basin and other sedimentary basins in Kenya (Heya, 2012).

Eames and Kent (1955) indicate that the depositional history of the Lamu Basin is characterized by distinct sandstone facies which formed from Permo-Carboniferous through Tertiary. It occurs in four megasequences that show variation in grain sizes, porosity, permeability, compaction, shaliness, and cementation (Mbede and Dualeh 1997). This is largely determined by the forces involved in the formation and their environmental setting. The facies categories include; continental rift basin sandstones, fluvial-deltaic sandstones, and the sandstones due to marine deposition (NOCK, 1995). Such tectono-eustatic pulsations during Tertiary may have conveyed source rock and reservoir formation in a spatial connection in which oil and gas could be trapped.

Hence, several of the wells drilled intersected good gas and oil shows; three wells flowed gas. The thick tertiary deposition conveys prospective source rocks into play as mature hydrocarbon sources. Migration pathways are postulated to be direct and relatively short. There are Tertiary and cretaceous depocentres in restricted marine settings within structural highs. Total Organic Carbon (TOC) of 11% and Hydrocarbon Index (HI) of up to 688 have been reported from Eocene source rocks from Lamu basin samples (Osicki et al., 2015).

Gravity data supports presence of oil "kitchen" troughs amid other prominent structural features of offshore Lamu basin as shown in figure 2.2 (Masinde, 2015).

Isostatic anomaly is usually used to offer a general structural image of an area by bringing out gravity variations. The low-density formations in blue show sediment fill in the basin while the high density formations in red illustrate shallow basement. Figure 2.2 is predominantly useful in interpreting vertical fault displacement, basin/sub-basin extent, and variation in deposited sediment quantity. Huge negative anomalies demonstrate thick sediment deposition and vice-versa.

Bosworth and Morley (1994) proposed that basement highs within continental shelf are an indication of possible Jurassic limestone or Karroo sandstone reservoir. Halokinesis of Mid-Jurassic salt deposits in Miocene period offers extra positive outlook in the offshore region. Paleogene deltaic sandstones occurring in interchanged listric fault slabs amid a Miocene reef play, coinciding with Eocene shale source rock is evident (Mbede and Dualeh 1997). Such information can be verified and or corroborated through well log analysis.

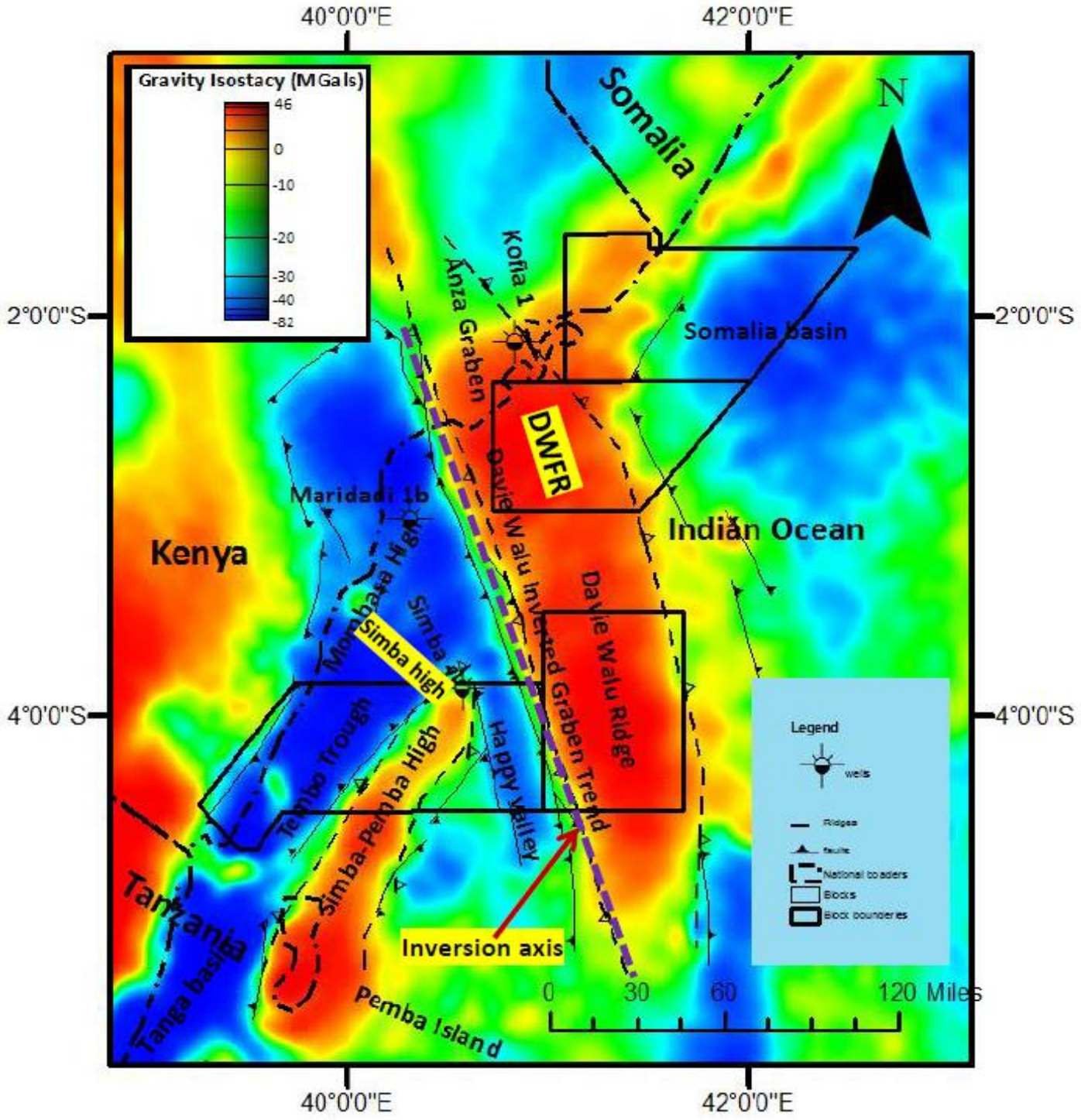

Figure 2.2: Isotactic gravity map with regional structural overlay (after Masinde, 2015).

2.4 Well Logging

Sensors used in logging tools measure certain physical properties of formation as they are pulled up the wellbore from a truck (Figure 2.3). These measurements recorded digitally, on magnetic tapes and printed on long paper strips are referred to as well log. It is possible to estimate petrophysical characteristics of the subsurface using geophysical well log information (Bassiouni, 1994). The number of log data available determines the accuracy and diversity of the estimates.

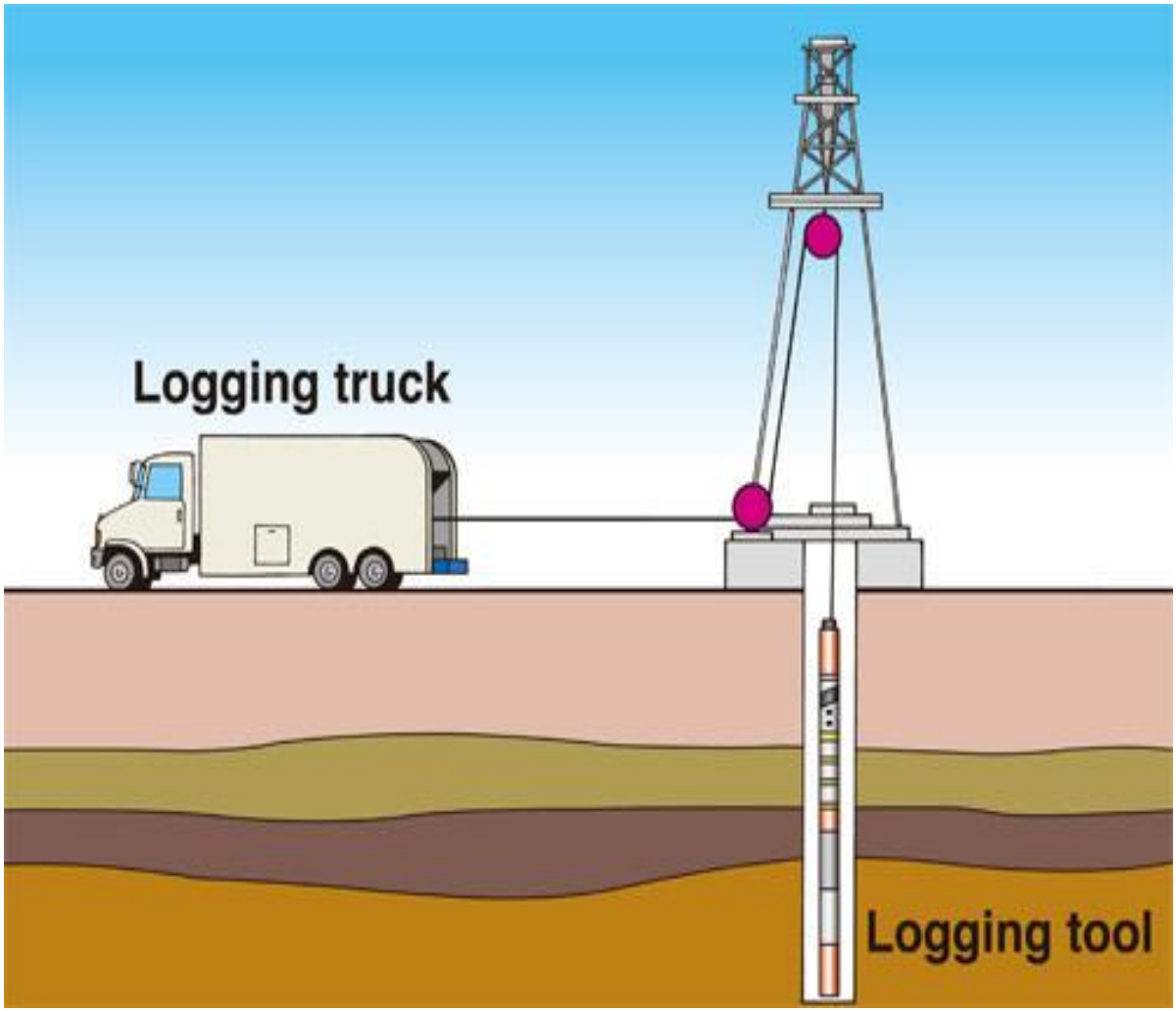

Figure 2.3: Schematic diragram of a loggging truck & equipment set up (modified Rider, 2002).

Today several different logs can be run including measured properties as intensity of natural radioactivity of rocks, conductivity or resistivity, velocity of acoustic waves, and electrical

potential existing in the wellbore. Logging tool characteristics vary such as depth of investigation, vertical (bed) resolution, and investigation geometry, among others (Figure 2.4).

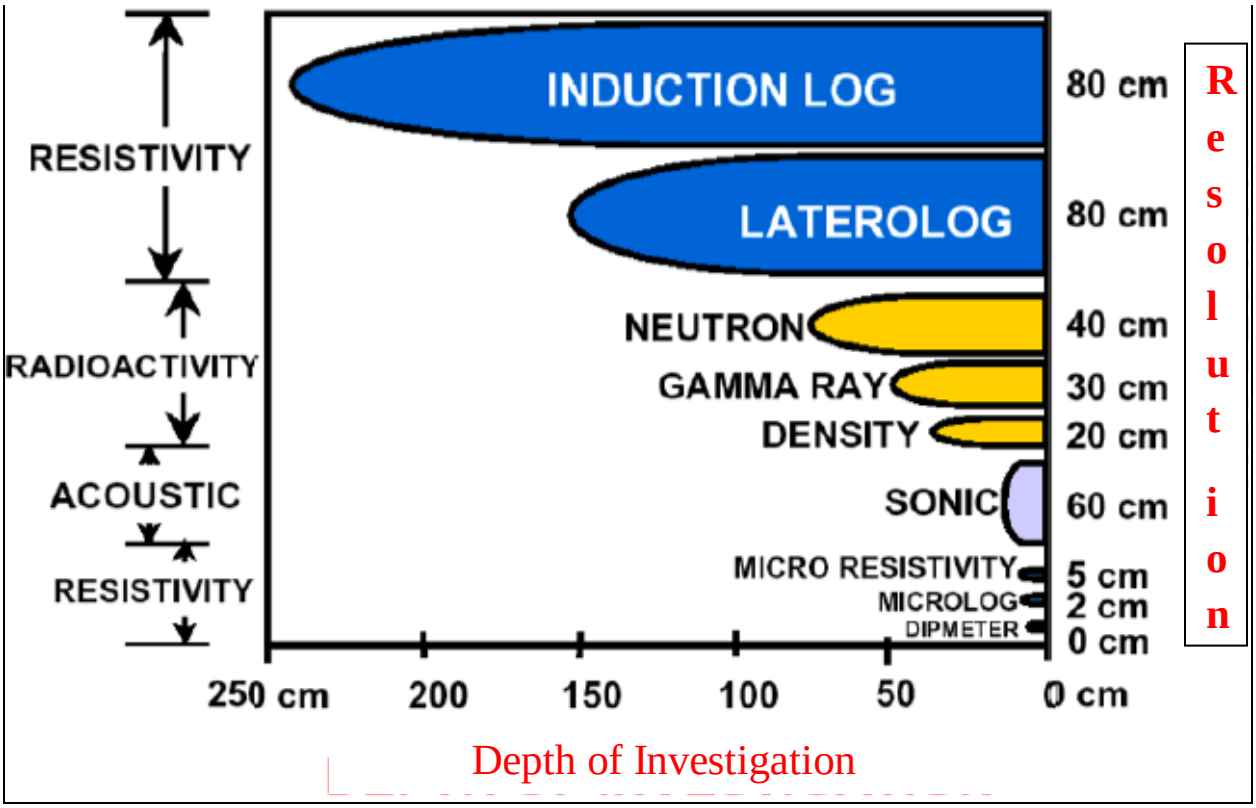

Figure 2.4: Depth of investigation and resolution for various logging tools (after Rider, 2002).

Interpreting well logs gives petrophysical parameters like porosity, fluid saturation, permeability, and lithology (rock-type). The log analyst is therefore tasked to utilize the collected measurements to establish the presence and volume of HCs in the well (Wyllie and Rose, 1950). In this research, nuclear well logs from three selected wells were analyzed to characterize and estimate hydrocarbon reserves through formation evaluation.

2.5 Formation Evaluation

The potential of the formation is evaluated in order to know the hydrocarbon in place. This requires knowledge on fluid saturation, porosity, and thickness. With limited direct measurements, the preceding parameters can only be inferred from indirect geophysical

measurements. Hence, formation evaluation is the science and "art" of taking multiple wellbore measurements (all of which are indirect) and constructing an integrated description of formation properties (Bloch, 1993).

Primary tools for determination of saturation, porosity and permeability are resistivity logs, acoustic logs, nuclear logs, and SP log (Table 2.1). Unlike the SP and resistivity logs, nuclear logs are advantageous because one can log through casing or gas formations, and they have better resolution. The final goal of formation evaluation is to assist establish the reservoir size, the volume of hydrocarbons, and the producing capabilities of the reservoir (Edmundson and Raymer, 1979). Exploration methods such as gravity, seismic, magnetic and geologic tools lead only to the initial discovery of a reservoir. Tiab and Donaldson (2004) argue that formation evaluation provides the means of gathering the information required for economic analysis and development planning.

Table 2.1: Logs and their chief application in formation evaluation (Kozhevnikov et al., 2011).

Petrophysical/ Geological Parameter	**Log Type**
Fluid saturation and porosity	Resistivity, Sonic, Density, Neutron
Shale content	SP, GR, Neutron, Density
Rock Type- Lithology	Sonic, Density, Neutron, GR
Permeability quantification	NMR, SP, Image logs
Reservoir thickness or net/gross	Well logs and seismic

From Table 2.1, it can be concluded that formation evaluation for petrophysical parameters can be achieved through the analysis of various nuclear well logs, rendering non-nuclear logs for correlation and or calibration. Note that the reservoir area needed in the calculation of reserves is usually derived from seismic.

2.6 Principles of Nuclear Logging Techniques

Okechukwu et al (2018) defines nuclear or radiation logging as a constant record of induced or natural radiation emanating from geological formation surrounding the wellbore. Equipment for radiation logging comprises of a detector or else a nuclear source and detector. The tool records electrical impulses originating from the radioactive detector (Okechukwu et al., 2018). The most popular wireline nuclear equipment are natural GR tool, density tool, and neutron tool, not omitting the latest, NMR. While the neutron and density devices necessitate the utilization of a radioactive source element, the GR tool is an inert system devoid of radioactive sources used for varied applications (Crucian et al., 2017).

According to Edmundson and Raymer (1979), nuclear logs are utilized in geotechnical site examinations to compare layers among boreholes, and assist in defining lithology. Some typical well logging tools and their sizes are available in appendices B. They are applied in HC exploration to deduce or indirectly estimate several geophysical properties of rock material, comprising of density, permeability, porosity, and fluid saturation (Desbrandes, 1985). Hence, this section provides a catalog of nuclear tools available to the log analyst. Included are: lists of the measurements made, units of measurements and major applications.

2.6.1 Gamma Ray Log Technique

A GR log records natural radioactivity in geological formations. Natural γ radiation occurs in rocks in varying quantities. Radioactive minerals such as U, Th, and K, are associated with diverse depositional environments (Kozhevnikov et al., 2011). Low γ radiation is characteristic of sedimentary carbonate and sandstone environments. Shale and clay formations show superior amounts of γ radiation. Thus, type of lithology can be positively indicated by GR log in “counts” or API units. The sources of natural radiation in rocks and their abundances are as shown in Table 2.2, which implies that each source contributes approximately the same amount of radioactivity.

Table 2.2: Relative abundance and contribution of radioactive elements to the overall radioactivity in rocks (modified from Rider, 2002)

Natural Gamma Source	Production rate photons/g/s	Relative Abundances %	Decay product
Potassium K^{40}	3	99.96	argon
Uranium^{238}-Radium series	26000	0.015	lead
Thorium series Th^{232}	12000	0.025	lead

Potassium is common volumetrically and chemically active in naturally occurring lithologies. It is bound chemically as a salt, in the clay silicate structure, and in rock forming minerals like feldspars. Hence potassium behavior can be viewed both in terms of chemical composition and radioactivity contribution. Since most shales contain a mixture of clay minerals (Illite with high K or smectite and kaolinite with low K), the difference in potassium content is muted. Thus, shale on average is composed of 3% potassium (Rider, 2002).

The principal original uranium source is the acid igneous rocks, as they contain 4.65µg/g of the element on average. Uranium forms soluble salts and an oxide that are transported in stream water. Perhaps the most common means of accumulating uranium into sedimentary rocks is in association with organic material. It has been proven through experimentation that carbonaceous matter can efficiently extract uranium from solution, particularly over the acidic range of pH 3.5-6.0 (Ellis and Singer, 2008). More often, organic rich shales possess high amounts of locally extracted (syngenetic) uranium, in which case they are linked with high GR log readings.

Thorium has its principal origin from intermediate and acid igneous rocks. Conversely, it is not soluble, and unlike uranium, it is extremely stable. This explains why it is found in residual soils (bauxites). Even though there are chances for thorium to be adsorbed on clay minerals, it is usually carried to sediment deposition sites in form of clay fraction detrital grains (Durrance, 1986). These are mostly of very stable and heavy minerals like thorite, epidote, monazite, sphere, and zircon (Rider, 2002). Regardless of the source of natural radiation, the GR equipment is utilized to detect the presence and intensity of the gamma rays.

The GR device entails basically of an extremely sensitive γ ray sensor, usually a scintillation counter. The detector consists of a NaI(Ti) (thallium-activated single sodium iodide) crystal supported by a photomultiplier (figure 2.5). The emitted gamma ray experiences consecutive Compton scattering impacts with electrons of rock formation, losing on energy. Only gamma rays with energy between 0.5-3 MeV are scattered by rocks before being absorbed (Figure 2.6). Standard gamma ray equipment records all gamma rays that reach the detector from any source. Since each type of decay is characterized by gamma rays of a specific energy, spectral GR tools measure the response in three energy windows. In sedimentary environment, the log usually reveals the shale content of the rocks since the radioactive elements tend to concentrate in shale (Heslop, 1974).

Owing to detector type variations, tool design, and efficiency, the American Petroleum Institute (API) standard is frequently used for calibration (Axelrod and Hearst, 1984). There is a test well in Houston, Texas that has been used for several years as the API reference standard well. GR log interpretation is performed based on the relatively high and low count rates linked to “dirty” and “clean” environments respectively. Formations composed of more shale or clay as shown by higher γ count rates are commonly extra strongly compacted with finer units and thus imply lower porosity and hence, less permeability.

Figure 2.5: A gamma ray (GR) equipment, the latest tools are of the same design but with larger crystals and enhanced sensitivity to gamma rays (courtesy of CBG Corp).

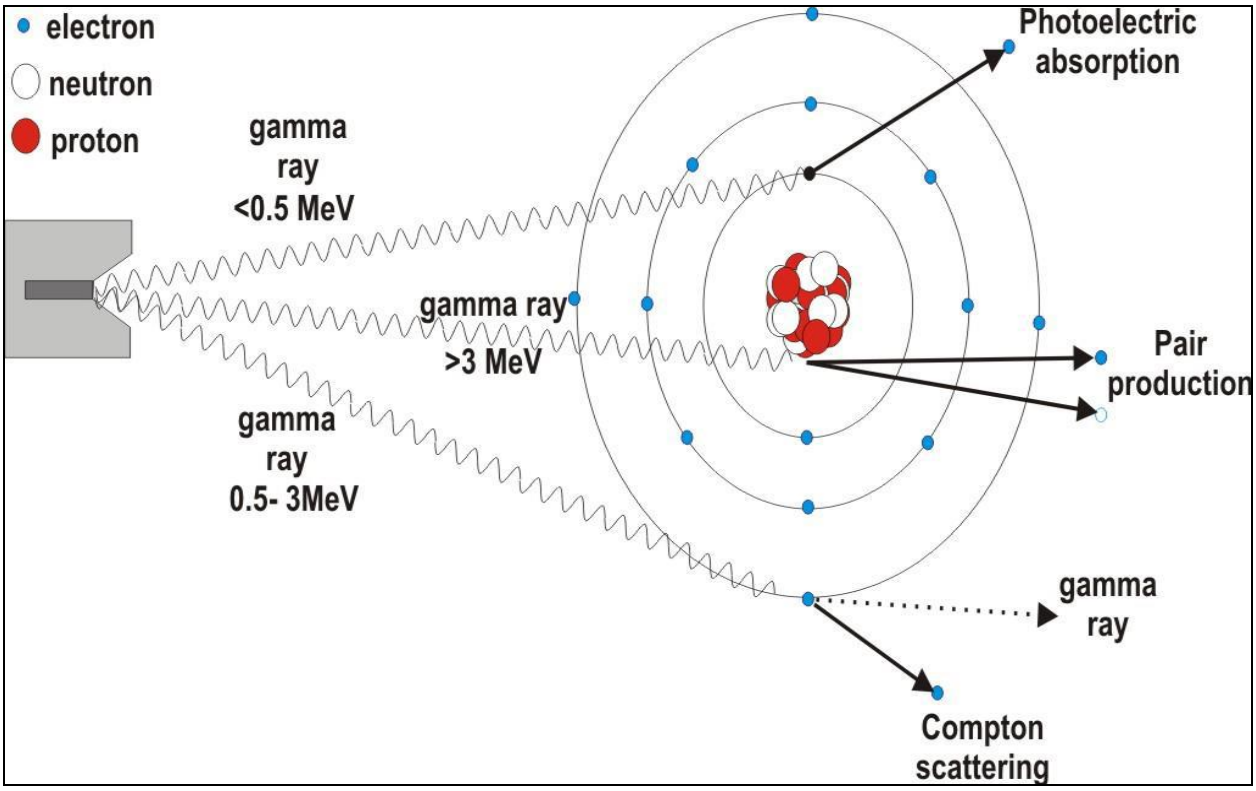

Figure 2.6: Principle for GR tool detector response-Compton scattering (after Podgorsak, 2005).

The GR log is important for depth control due to unavoidable mix up of cuttings and the high cost implication of cores. Furthermore, GR has better vertical resolution compared with SP log. However, potassium chloride (KCl) based drilling muds increase gamma ray throughout. Other additives such as barite used to increase mud weight, reduce viscosity of mud, and control fluid loss affect the GR and density log because they are highly absorbent. Mud type, additives and salinity ought to be known so that appropriate corrections are made in the readings.

2.6.2 Neutron log Technique

Neutrons are electrically neutral units whose mass approximately matches the mass of the hydrogen atom. Neutron sources use two elements; an alpha (α) radiation source such as americium, plutonium, or radium, and beryllium-9. The Am-Be neutron source in the sonde continuously emit (Zhao et al., 2015) high energy neutrons (≥ 0.5 MeV) based on formula 2.1.

$${}^{9}_{4}Be + {}^{4}_{2}He \Rightarrow {}^{12}_{6}C + {}^{1}_{0}n + \gamma \quad \text{.....} \quad (2.1)$$

Mheluka and Mulibo (2018) state that neutrons ram into nuclei of rock atoms, and lose energy via billiard-ball like collisions before they are detected. Detectors are based on n + 3He → 3H + 1H + 0.764 MeV reaction (Schlumberger, 1989). 3He is target and proportional gas counter for thermal neutrons. For epithermal neutrons, a detector is covered by a cadmium sheath to absorb thermal neutrons.

The neutron log offers a record of the lithology's reaction to bombardment by fast neutrons. It is expressed in form of *neutron porosity units*, which are linked to hydrogen index (HI), a pointer to the formation's hydrogen richness. Dunn et.al (2002) and Farag (2010) define the hydrogen index as the quantity of hydrogen per unit volume of a fluid divided by the quantity of hydrogen per unit volume of pure water in standard conditions, that is;

$$HI = \frac{amount\ \ of\ \ hydrogen\ \ in\ \ sample}{amount\ \ of\ \ hydrogen\ \ in\ \ an\ \ equal\ \ volume\ \ of\ \ pure\ \ water} \quad \text{.....} \quad (2.2)$$

Where HI of water=1 based on Yang and Hirasaki, (2008).

Nevertheless, quantitatively the oilfield interest in hydrogen is as a porosity indicator and fluid filler. The neutron log shows the HI which in most cases is converted to *neutron porosity units* (45 to -15). Qualitatively, the neutron log is an exceptional discriminator between gas and oil. On their own, the density and neutron log are challenging to apply as a gross lithology identifier. When combined on a compatible scale, the logs offer one of the excellent subsurface lithology pointers obtainable (Ellis and Singer, 2008). This is because both show the same formation parameter-porosity.

Neutron logs are primarily used for porosity and lithology determination. The equipment responds to the quantity of hydrogen around the wellbore. Hence, in clean (clay-free) geological material with oil or water filled pores; the neutron kit response is a reflection of the volume of fluid-filled porosity. It is possible to distinguish gas zones from oil or water zones by matching the neutron data over some other porosity log (Ransom, 1977). An appropriately calibrated

neutron tool (typically to the API standard) affords essential data on formation rock composition. Figure 2.7 gives a general view of the modern neutron tool.

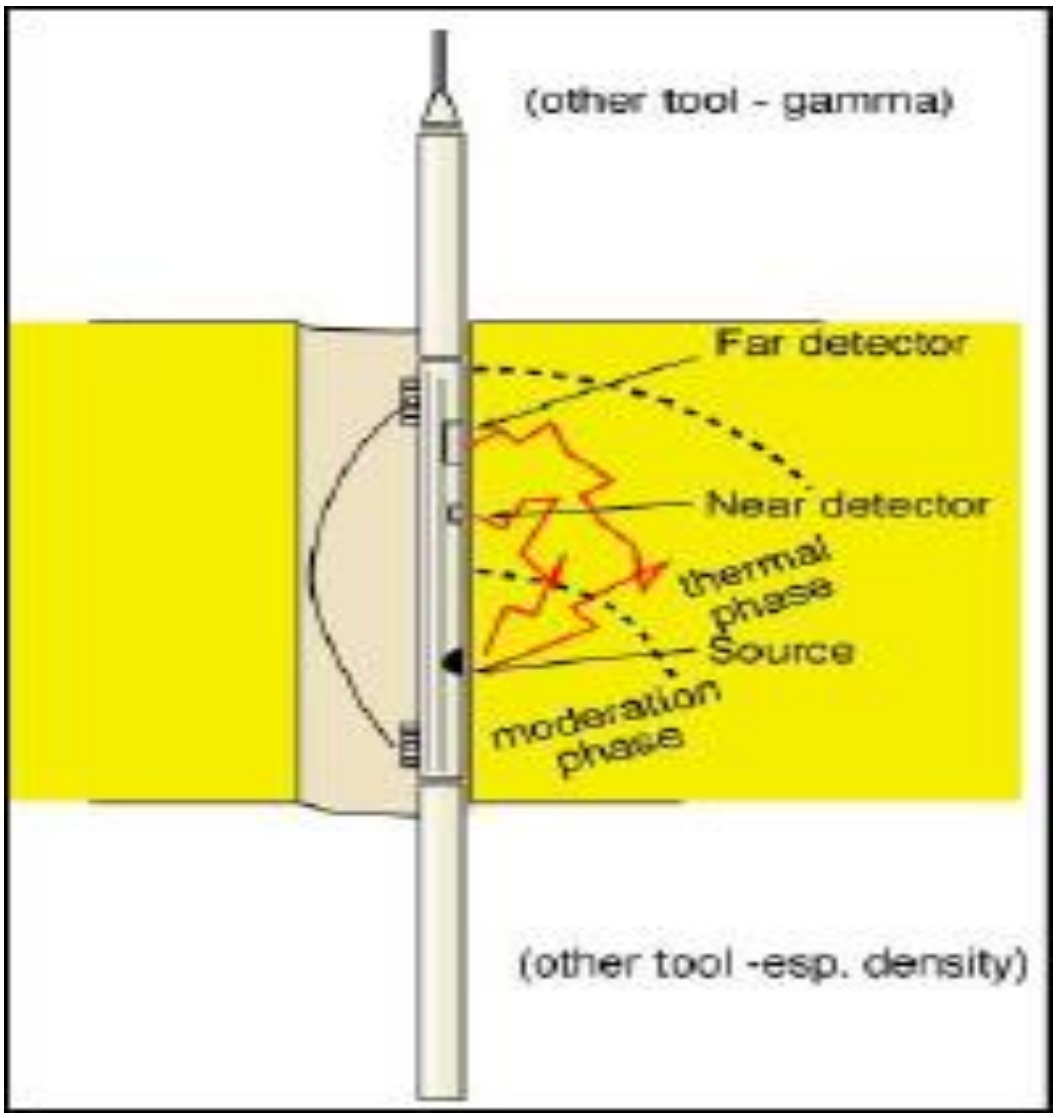

Figure 2.7: Neutron tool set up (adapted from Nelson and Mitchell, 1991)

The neutron tool is usually positioned above the density sonde, hence logging the formation first, as the gamma bombardment used by the density equipment could disrupt the neutron tool values (Rider, 2002). Measurement depends on the type of neutron logger, either measures epithermal neutrons or capture gamma rays. The two detectors are used to calculate the ratio of counts. If hydrogen content is high, most neutrons will be slowed down and captured in a short distance. Water and oil have similar H_2 content, hence response to liquid filled porosity. Gas is much less

dense, and so depicts an underestimated porosity. Slowing of neutrons is less with gas relative to water – low Φ. The tool is sensitive to chloride absorption, hence need for corrections and eccentring. Standard logging speed for the GR, density and neutron tool is about 1300 ft. /hr (400 m/hr).

2.6.3 Density Log Technique

Density devices employ a chemical source of gamma radiation (Cs-137; $T_{1/2}$ = 30.2 yr; E_γ = 663 keV) and two gamma ray detectors to determine the formation bulk density (Figure 2.8). The two receivers - one at a shorter distance (7") is used to compensate the other at a longer distance (16") for borehole effects.

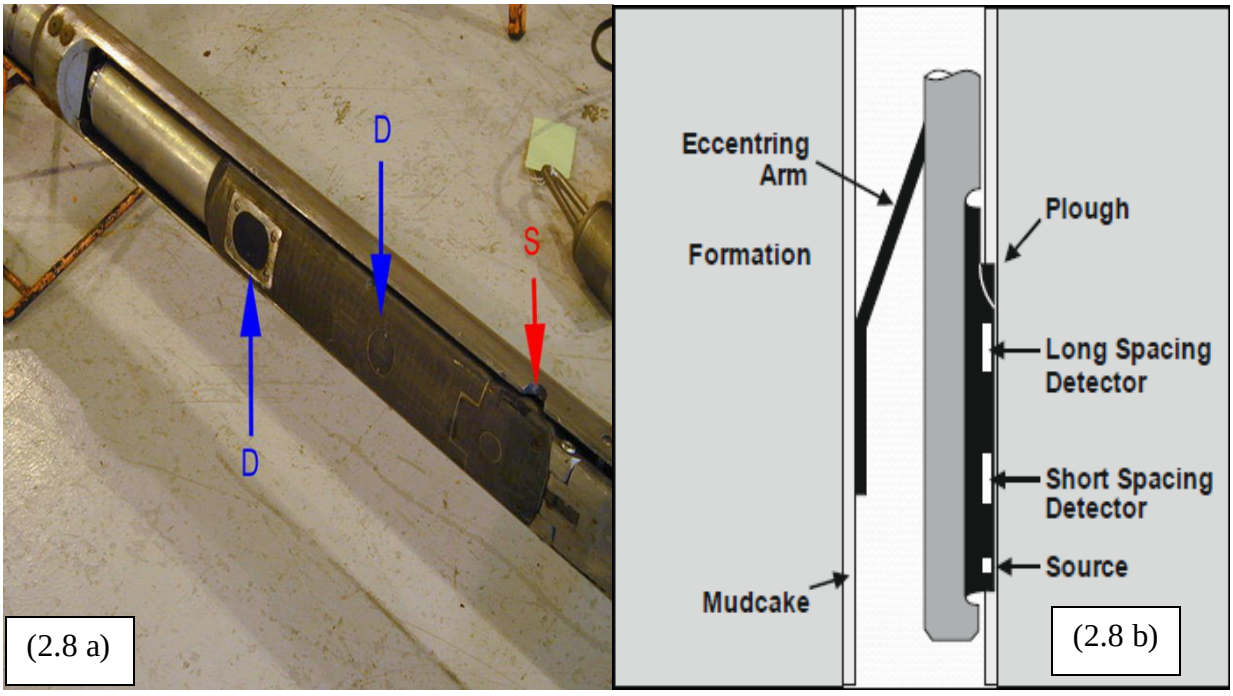

Figure 2.8: a) Density tool b) schematic logging setup (after Baker-Hughes-Atlas, 2002)

As gamma rays travel from the source (S) to the detectors (D), they are attenuated when they collide with electrons present in materials (rock) in their path through Compton scattering (Podgorsak, 2005) as illustrated in Fig 2.6. The attenuation is largely a function of the electron densities of those materials, which are formation matrix and pore fluids. Adsorption and attenuation of energy in backscattered gamma rays can be used as an indication of electron

density. There is good correlation of electron density and bulk density in most formations safe for gypsum, salt, and coal. Recording is done in counts/second. Statistical fluctuations are not a problem since gamma ray intensities are larger than the GR tool. Nonetheless, logging about 1300ft/hr or less allows recording of a significant number of counts per second. The tool is sensitive to barite muds since they are very absorbent and can ruin the measurement.

Erroneous porosity values may be computed when there are changes in fluid density, especially when the formation is saturated with gas. The presence of gaseous hydrocarbons causes dramatic drop in fluid density, leading to a too high porosity on the density log. In the presence of oil, the density log gives an essentially correct porosity (Kozhevnikov et al., 2011). This happens because of the fact that oil and water have nearly the same density, and the tool investigates the flushed zone that normally retains a small volume of oil. However, gas is more mobile and occurs frequently in the flushed zone, where due to the large difference in density with respect to water, results in diminishing the bulky density as pronounced above. Compensated density tools measure in-situ bulk formation density and compensate the measurement for borehole invasion (mudcake) effects.

The log is presented in bulk density (g/cm^3) and incorporates an adjustment curve that specifies the degree of rectification (compensation) subjected to the bulk density measurement (Baker-Hughes-Atlas, 2002). The densities of common rocks are seldom diagnostic because we have excessive overlap and too much spread due to disparities in texture and composition. In general, oilfield densities often range between 2g/cc and 3g/cc, with common lithologies (Table 2.3) spanning this scale.

Density measurements are primarily used to calculate formation porosity when lithology is known. When combined with other porosity logs, density log data is used for the detection of gas, evaluation of shaly sand, and identifying lithology. Finally, density log data can be calibrated through routine core porosity results. Nonetheless, modern advances in specialized logging techniques and in particular NMR log have led to directly inferring or measuring permeability.

Table 2.3: Densities of typical oilfield lithologies (after Rider, 2002)

Lithology	**Range** (g/cm3)	**Matrix** (g/cm^3)
Sandstone	1.9-2.65	2.65
Shale-clays	1.8-2.75	Varies ~2.65
Limestone	2.2-2.71	2.71
Dolomite	2.3-2.87	2.87

2.6.4 Nuclear Magnetic Resonance Technique

The Nuclear Magnetic Resonance (NMR) is similar in technology to the medical MRI (Magnetic Resonance Imaging) scan, both of which became popular in the 1990's due to a new generation of tools. The tool is based on the principle that hydrogen protons possess a great magnetic moment and behave like miniature spinning magnets aligned to the direction of the Earth's magnetic field (Liu, 2017). A series of radio frequency pulses are used to tilt the protons by changing the field by 90^o with a signal of the same frequency as hydrogen, thus maximizing the response (Jackson, 2001). The protons then precess/spin in this new field like gyroscopes in a gravitational field. This precession is recorded by the equipment as a series of decaying spin-echo amplitudes.

The protons spin at slightly different frequencies due to small instabilities in the field, and lose energy – decay time T_2 (Dunn, et al., 2002). The initial maximum amplitude of the received signal is proportionate to the formation porosity. The decay rate of the obtained signal is associated with molecular exchanges happening in the fluid and is related to pore size and grain size distribution. Analysis of this information gives the fractions for: clay-bound water (CBW), capillary-bound water (BVI), and producible fluids (BVM) as illustrated by (AlRuwaili, 2005). Ultimately, NMR aims to distinguish between producible fluids and irreducible water, to be precise, permeability. Abouzaid, et al (2016) argues that NMR simplifies the assessment of shaly sands where low resistivity values often mask considerable hydrocarbon accumulation.

2.7 Summary of Literature Review

Essentially, every subsurface well drilled in the search for petroleum is logged with probes lowered into the wellbore to measure rock properties surrounding the hole. Logging offers a fast, comprehensive and economical investigation of the whole length of the drilled well.

Nuclear logging techniques are commonly used in the mineral industry and are starting to be applied to evaluate the commercial viability of hydrocarbons (Rider, 2002). Nuclear well logging was presented on a commercial scale to the petroleum industry in 1950 for detection of different rock types and estimating the porosity. Many of the initial radioactive well logging tools used was developed on experimental results acquired in boreholes.

However, in recent years, several research programs have focused to investigate the essential processes when radiation penetrates sedimentary rocks, common earth elements, and formation fluids in the wellbore have been carried out (Ellis and Singer, 2008). Consequently, these investigations conducted in various countries have led to major developments in nuclear logging. This research aims to apply nuclear logging developments in hydrocarbon reservoir characterization.

As stated earlier, nuclear well logging has played an important role in the past half century in the detection of hydrocarbons and complements other traditional techniques; core drilling for determining rock formations, rock cuttings to provide information on the existing lithology, and acoustic technique for density determination (Kozhevnikov et al., 2011). Even coring, that is ordinarily ridiculously expensive gives scanty data on formation fluids, besides the fact that Total Core Recovery (TCR) rarely gets to 100 percent.

However, unlike resistivity and spontaneous potential (SP) tools, the nuclear methods have the ability to log formations filled with gas or air as well as through steel casing. In addition, determination of petrophysical parameters is necessary to characterize the development of hydrocarbon reservoirs.

CHAPTER THREE: METHODOLOGY

3.1 Introduction

This section describes the various concepts used in the quantitative analysis of well log data in this study. The chapter also highlights the basic techniques and procedures used, for determining the petrophysical parameters of interest in this study.

Figure 3.1 shows the location of the study area in offshore Lamu basin

3.2 Description of the Lamu Basin and sampling for petrophysical parameters

Lamu Basin is the largest HC prospective basin that covers both onshore and offshore south eastern Kenya. The geology of the basin consists of potential source rocks (shale) and sandstone reservoirs. A number of wells drilled prior to the year 2018 within Lamu basin had oil and gas shows, but no commercial hydrocarbons were declared. It is from this group of exploration wells that Kofia-1, Simba-1, and Maridadi-1B were identified for this project (Figure 3.1).

Geophysical well logs from the three wells were subjected to petrophysical analysis to gauge the HC potential of offshore Lamu Basin.

The main geophysical data considered in this research are gamma ray log, neutron log and density log. In addition, non-nuclear techniques such as SP, caliper, sonic, and resistivity logs were used whenever available, for correlation and validation.

Appendices C1-C3 shows the schematic drilling well geometry adopted for the three wells considered in this study, at different geological formations at the well location in the field. The schematics show the seabed where drilling commenced, reducing casing hole diameters with depth (for well stability and formations present) and the maximum depth reached for the three wells.

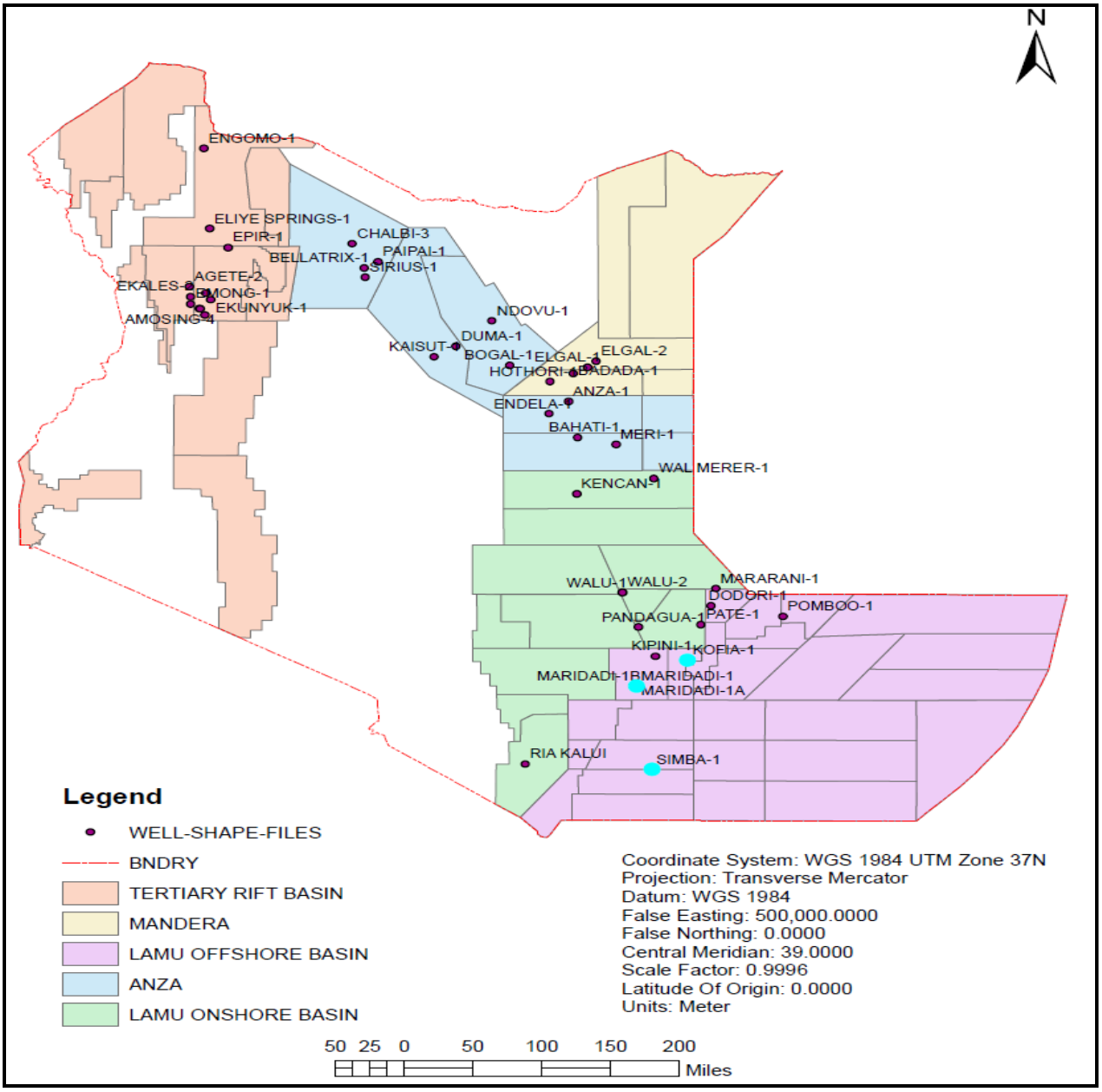

Figure 3.1: Location of exploration wells in Lamu Basin whose data were used in this study.

Table 3.1 shows the summary of the drilling profiles of vertical exploratory wells studied in this project. Three types of drilling fluids were used, namely; KCl polymer for Kofia-1, natural sea water for Maridadi 1B and barite muds for Simba1. In principle, KCl increases gamma ray counts, emitted from the natural radioactive ^{40}K while barite muds affect the GR and density log because they are highly absorbent. Additives are used in order to increase mud weight, reduce viscosity of mud, and control fluid loss. Hence prior corrections are made on the log readings.

Table 3.1: Basic well data of Lamu Basin exploratory wells

	Kofia-1	**Maridadi-1B**	**Simba-1**
Water depth (m)	94	39	921
Total depth (m)	3657	4197	3604
Duration (days)	95	89	112
Drilling fluids	KC*l* polymer mud	Sea water & mud slugs	Barite muds /slug
Well Logs	GR, LLS, LLD, RHOB, NPHI, CAL	GR, LLS, LLD, RHOB, NPHI, CAL	GR, LLS, LLD, RHOB, NPHI, CAL, SP, SONIC

Eight (8) geophysical logs were used in this study for petrophysical analysis, namely; gamma ray (GR), deep resistivity (LLD), density log (RHOB), caliper log (CAL), neutron log (NPHI), shallow resistivity (LLS), spontaneous potential (SP), and sonic log.

3.2.1 Sampling for petrophysical parameters

Figure 3.2 and 3.3 shows the equipment used in nuclear data logging.

The nuclear logging equipment used were calibrated in quarried limestone/sandstone/dolomite blocks with a range of known average porosities and densities, done at the University of Houston, Texas, one for neutron-porosity tools, and another for natural-gamma logs, prior to measurements.

The standard calibration conditions for this equipment were: $7\frac{7}{8}''$ borehole diameter; fresh water in wellbore; No mud-cake; eccentered hole; 75° F temperatures; and standard atmospheric pressure. Any departure from the aforementioned conditions requires corrections (Baker et al., 2015).

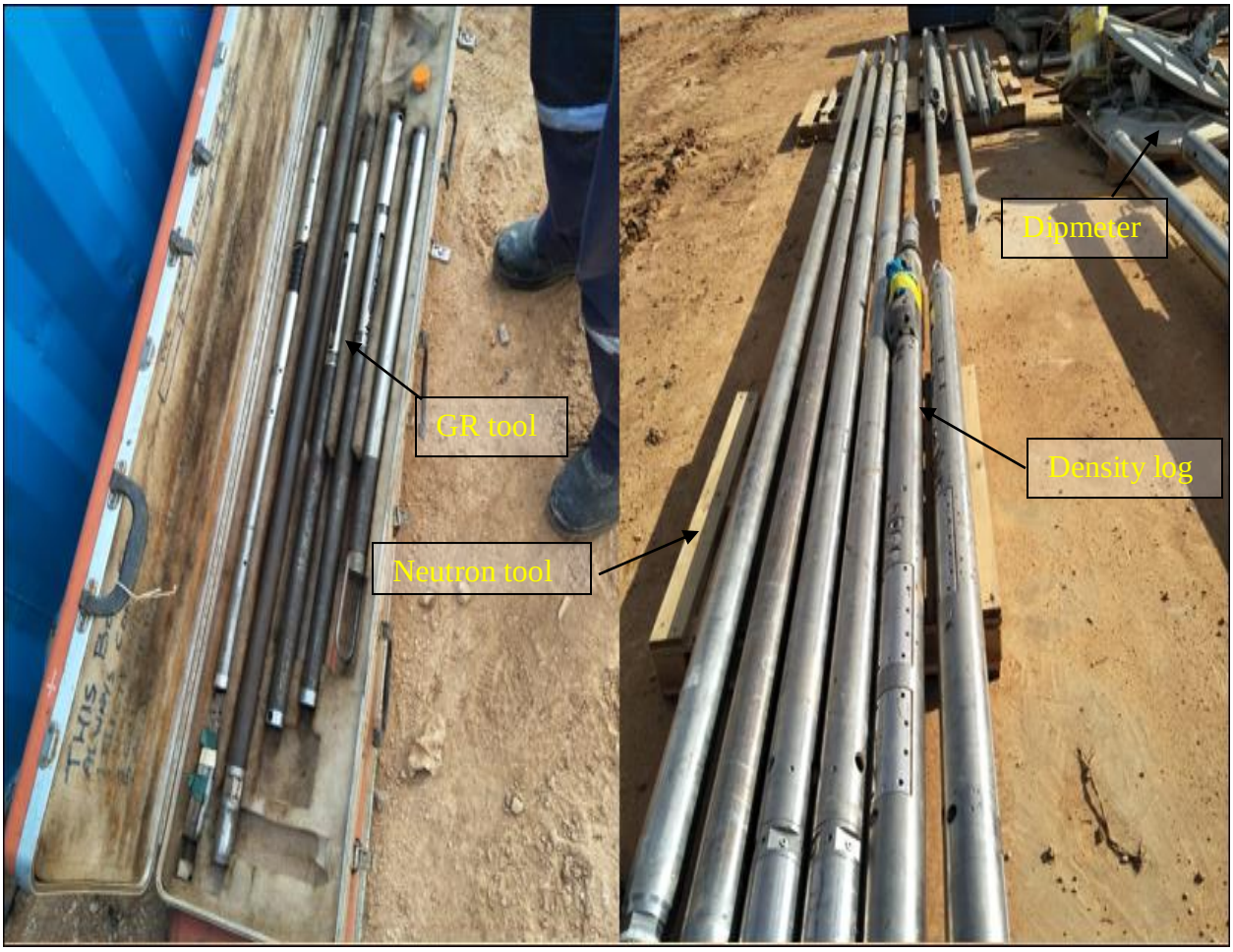

Figure 3.2: Equipment used in nuclear log data acquisition (Halliburton, 2017)

The neutron log was calibrated to measure porosity scale (−15 % to 45%). Our measurements were done within the validity of the equipment calibrations period, three (3) months, later at the offshore Lamu Basin.

The logging equipment were connected together in the standard gamma-neutron-density arrangement and lowered to the depth of the wells. The sonde was pulled up at a speed of approximately 400 m/h and readings recorded after every 4 ms -5 ms, after corrections for background counts. To eliminate the influence of thermal neutron effects on the data, only neutrons and inelastic gamma rays within a certain energy window were measured.

The real-time display of data was monitored on the LCD screens, allows for quality control checks and data acquisitions for later processing for petrophysical parameters data.

Figure 3.3: Display of log data acquisition and monitoring screens in the logging truck (Hulliburton, 2017)

The data in LAS format was viewed in the compatible notepad++ prior to being displayed in Techlog software. Appendix C4 shows nuclear log data in LAS format for Maridai-1B.

The following assumptions form the basis of quantitative log interpretation during this investigation:

a) Reservoir formation (sandstone/limestone) regarded to be lithologically clean
b) Beds below 1m thick are regarded to be thin, thus not incorporated during analysis.
c) Pore fluid is either water, hydrocarbon (gas/oil), or both and
d) Connate or formation water is saline

3.3 Determination of petrophysical parameters

This analysis utilized log data to offer an understanding of the subsurface geology at the well location and formation response to these reservoir qualities (Ellis and Singer, 2008). Therefore, standard formation evaluation techniques were used to derive lithology (V_{sh}), water saturation (S_w), porosity (ϕ), and to some extend permeability (K). The flushed zone technique was utilized to identify HC bearing zones within the reservoir of the wells studied where resistivity of mud fluid was in the header log. A combination of resistivity and GR log curves was employed to delineate hydrocarbon bearing zones in the study wells. In zones with hydrocarbons, the deep resistivity log (LLD) will exhibit high value readings since hydrocarbons have high resistivity as compared to salty formation water.

The water to oil saturation ratio was calculated to determine the presence and movability of hydrocarbons (Schlumberger, 1989), according to equation 3.1.

$$\frac{S_w}{S_{xo}} = \left[\frac{\frac{R_{xo}}{R_t}}{\frac{R_{mf}}{R_w}} \right]^{\frac{1}{2}} \quad \text{.....(3.1)}$$

Where: R_t is true resistivity, R_{mf} is resistivity of mud filtrate, S_{xo} is water saturation at flushed zone and R_{xo} for resistivity of flushed zone (Assaad and LaMoreaux, 2004).

The ratio S_w/S_{xo} was used to identify hydrocarbon bearing zones and if they are moveable. In case S_w/S_{xo} =1, then no hydrocarbons can be moved despite the formation contents. Where S_w/S_{xo} value is approximately 0.7 or less, then movable hydrocarbons are present.

3.3.1 Volume of shale (V_{sh}) determination

The Gamma Ray (GR) log is used to delineate shale beds whenever the SP data is distorted. The GR profile is a reflection of the shale proportion, hence can be quantitatively applied as an indicator of in several regions. Formation boundaries were picked midway between minimum and maximum deflection points of the anomaly. Schlumberger (1987) underlines the various ways of determining the V_{sh} in a zone or region. The following considerations were used to estimate V_{sh} in the shaly porous zones from the GR log deflections.

a) GR reading of the region of interest GR_{zone}
b) GR reading from a clean shale-free zone GR_{clean}
c) GR reading from 100% shale zone GR_{shale}

The shale fraction in the region of interest was then calculated:

$$V_{sh} = \frac{GR_{zone} - GR_{clean}}{GR_{shale} - GR_{clean}} \quad \text{.....(3.2)}$$

3.3.2 Lithology identification

Besides the GR log, combing the neutron-density logs on a compatible scale is the utmost lithology indicator for most rock formations. Evaporites and shales can be identified, matrix and clean formations can be suggested, and unusual minerals can be located with high probability. Ultimately, cross plotting of compatible logs can be used quantitatively to identify lithology. A large negative separation is a pointer to 'gas effect', which indicates presence of gas in the formation since slowing of neutrons is less with gas relative to oil or water (Rider, 2002). The standard density-neutron crossover was also used to identify lithologies based on Figure 3.4.

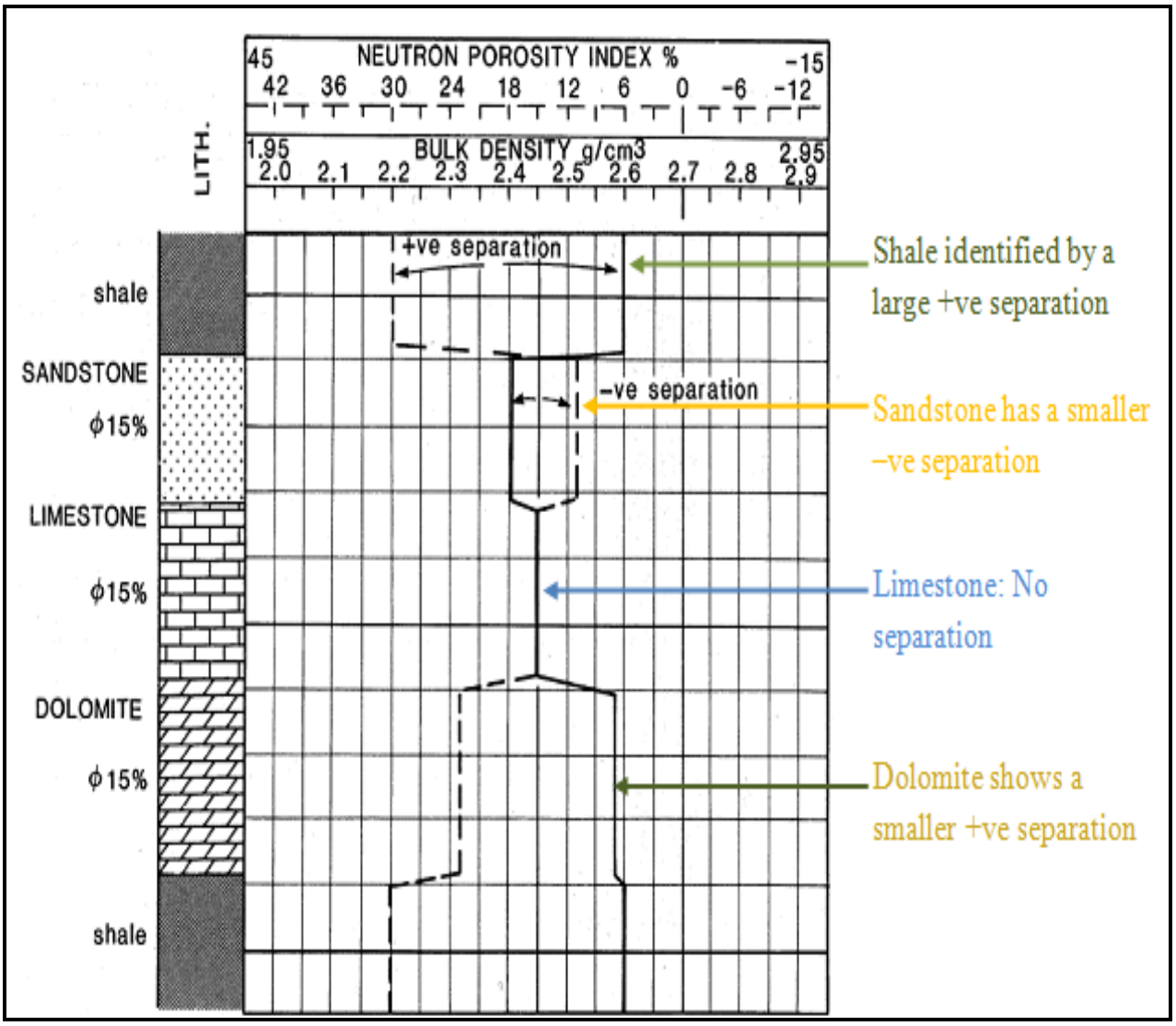

Figure 3.4: An ideal neutron-density log response for lithology identification (Rider, 2000)

3.3.3 Porosity computation

Individual porosity computation was achieved based on the formula 3.3 with the knowledge of various parameter densities.

$$\phi = \frac{\rho_{ma} - \rho_b}{\rho_{ma} - \rho_f} \quad \text{.....(3.3)}$$

Where: ρ_{ma} is density of matrix, ρ_b is bulky density, and ρ_f is density of fluid present

However, cross-plots are a suitable means in demonstrating how various log combinations respond to porosity and lithology. In addition, they offer visual insight on the usefulness and capabilities of different combinations. Examples of these combinations are presented in charts CP-3 through 19 (Schlumberger, 1987). The most effective method for determining porosity is the Density-Neutron cross-plot. This method was applied to compute porosity and mineral combinations in the Lamu Basin wells as exemplified in figure 3.5. The diverse porosity logs respond differently to fluid and mineral combinations. Therefore, the neutron-density cross-plot or other different porosity logs can be utilized to identify lithology/mineral proportions.

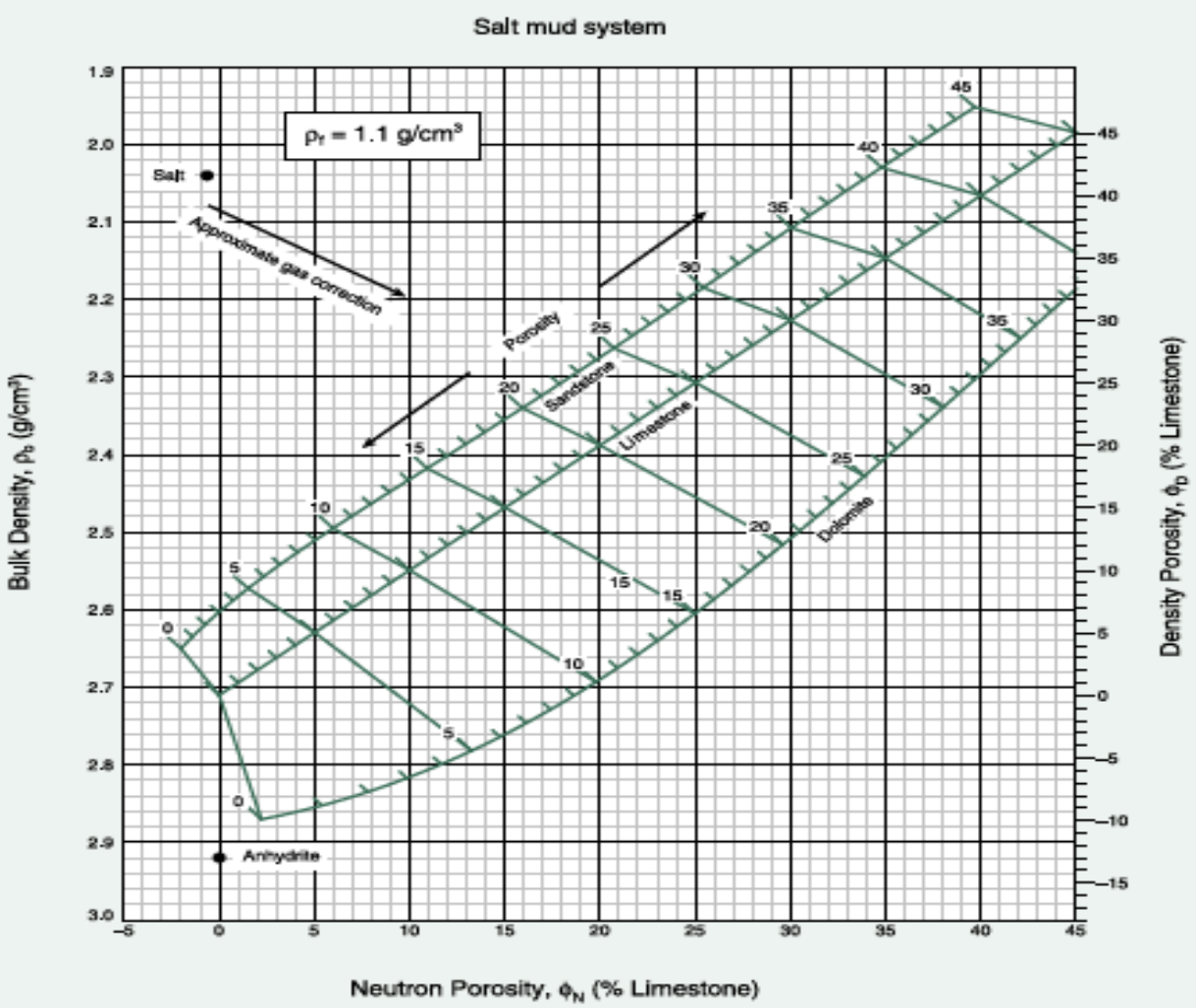

Figure 3.5: The density-neutron cross-plot, needed to find real, clean formation porosities due to the various effects of matrix type on the two nuclear logs (from Schlumberger, 1987)

From Figure 3.5, a point for a gas-free, monomineralic and clean formation will fall on one of the lithology lines, with its true porosity indicated based on line graduations. If the lithology of the reservoir is sandstone, graduations in porosity are chosen from the sandstone line matrix. Neutron porosity is lowered if gas is present, and hence gas-bearing zones have a propensity to plot above the matrix line of sandstone. Consequently, provisions for gas corrections were applied where necessary, by projecting points onto the suitable sandstone matrix to determine porosity.

3.3.4 Determination of Fluid Ssaturation

Formation, interstitial or connate water, is the uncontaminated water free of interaction with drilling mud or fluids. Water resistivity (R_w) is a vital interpretation element because it is needed in determining saturations from resistivity log (Wylie and Rose, 1950). However, there was no water catalogue, or chemical analysis to provide information on formation water resistivity of the study area. Thus, R_w was computed from resistivity-porosity cross plots and calculations based on equation 3.4, or from SP log where available.

$$R_w = \frac{R_t}{F} \quad \text{.....(3.4)}$$

The formation factor (F) is calculated from porosity while true resistivity (R_t) value is read from the deep resistivity log (LLD). This method is best suited for intervals where formation water resistivity is constant or varies only gradually (Morris and Brigg, 1967). Luckily, that happens to be the case in most hydrocarbon bearing regions, especially at depth. Nonetheless, due to significant lack of formation water flow during drilling, R_w was estimated from the SP log where available.

The fraction of pore volume in a reservoir formation that is composed of water is referred to as water saturation (Assaad and LaMoreaux, 2004). Unless otherwise stated, it is generally presumed that hydrocarbons fill the pore volume devoid of water. Ultimately, the determination of fluid saturation is one of the main purpose in well logging (Rider, 1996). Water saturations in clean and porous formation were determined based on Archie's formula and deviations thereof.

$$(S_w)^n = \frac{FR_w}{R_t} \quad \text{.....(3.5)}$$

Where n is a saturation exponent normally assumed to be 2, and F is formation factor calculated from the resultant porosity based on the equation 3.6.

$$F = \frac{a}{\phi^m} \quad \text{.....(3.6)}$$

For the sandstone in Lamu Basin the Humble formula was utilized to F where the constants a = 0.61 and m = 2.15 were used (Nyaga, 1995). Archie's S_w (water saturation) equation was also applied to compute fluid properties such as saturation.

A value for irreducible water saturation (S_{wi}) was also determined, by plotting porosity verses S_w (excluding values from transient and water zones), and getting the best fit of the data (Threadgold, 1971). The S_{wi} for any region can be computed by substituting effective porosity values in equation 3.6 (Shlumberger, 1989).

3.3.5 Permeability Estimation

The empirical relationship between tortuosity and fluid flow was initially stated theoretically by Tixier (1949), and later expounded upon by Wyllie & Rose (1950) for quantitative log interpretation. On the basis of Wyllie's general expression, numerous researchers recommended a number of empirical relationships for estimating permeability from irreducible water saturation and porosity derived from well log interpretation. Hence, one of such empirical relationships was applied in this study to estimate absolute (intrinsic) permeability (K) for oil and gas, as shown:

$$K_{oil} = \left(\frac{79 \times \phi^3}{S_{wi}}\right)^2 \quad \text{.....(3.7)}$$

$$K_{gas} = \left(\frac{250 \times \phi^3}{S_{wi}}\right)^2 \quad \text{.....(3.8)}$$

The recommended permeability for the product of porosity and water saturation in clean sandstone ranges between 0.08 - 0.12 mD (Crain, 1986). The empirical relationships have been improved with time, culminating in the relationship presented in Figure 3.6.

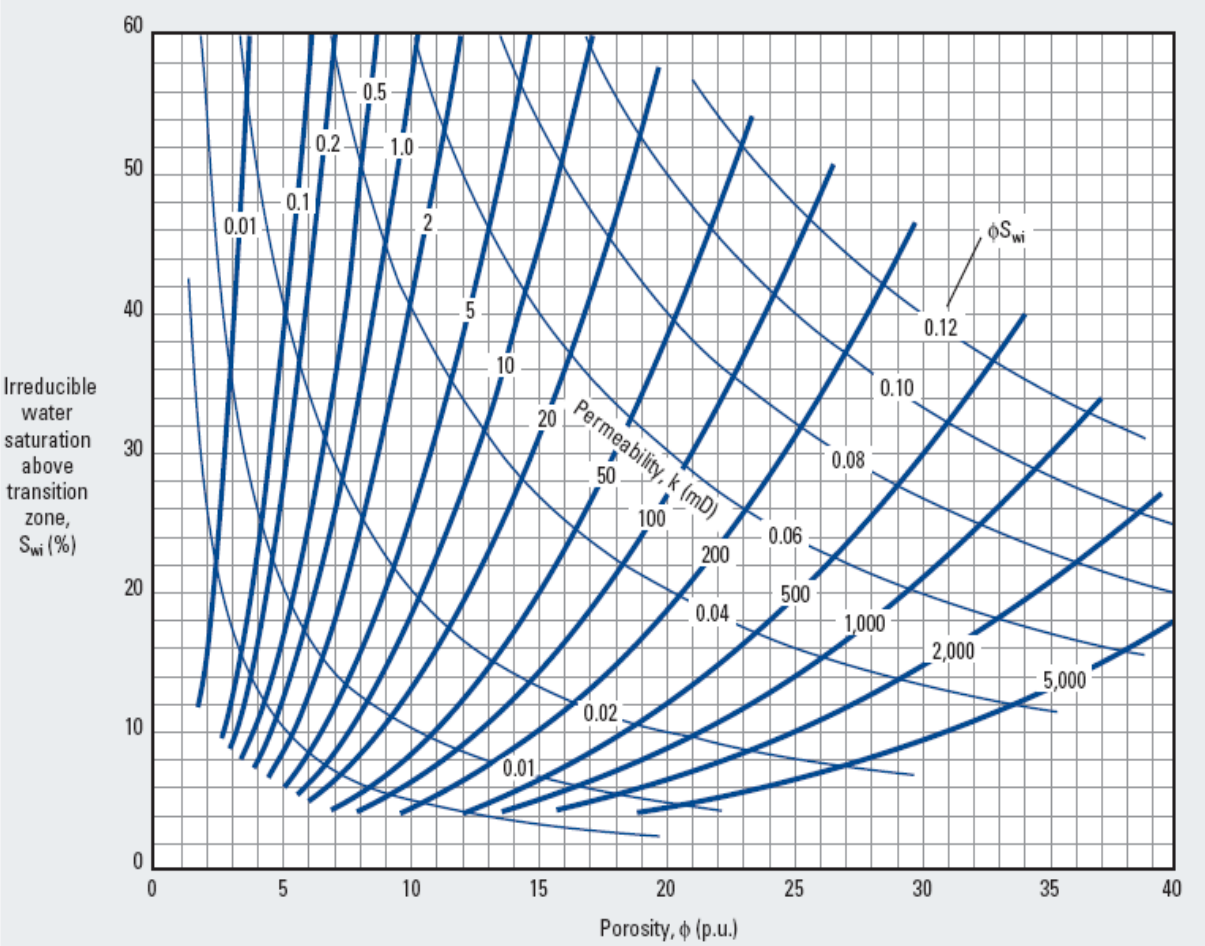

Figure 3.6: Computing permeability from porosity and water saturation (Schlumberger, 1987)

3.4 Estimation of Hydrocarbon Content

The term reserves describe the volume of hydrocarbons anticipated to be economically recoverable from recognized accumulations. Total reserve approximations encompass a certain degree of uncertainty depending largely on the volume of dependable engineering and geological information available and the interpretation of the same (Martin and Colpitts, 1996). The key petrophysical parameters required in reservoir evaluation are area, thickness, hydrocarbon saturation, and porosity (Dewan, 1983).

$$HCIIP = k.\phi.(1 - S_w).h.A \quad \text{.....(3.9)}$$

Where:

- HCIIP-hydrocarbons initially in place
- $(1\text{-}S_w)$ is the hydrocarbon saturation;
- *k*-constant units: 43560 for gas in SCF, and 7758 for oil in barrels
- *h*-productive interval (thickness)
- A-drainage area

Furthermore, the formation temperature and pressure control the mutual solubilities and viscosities of water, oil, and gas, (Krygowski and Asquith, 2005). The absence of individual well data about the reservoir area led to the failure to calculate the hydrocarbon reserves in place for the wells under study. Quantitative computations of fluid saturation (oil and gas) were also predicted based on apparent water resistivity logs rather than formation water resistivity due to absence of data on the latter.

Two core statistical techniques were applied in nuclear log data scrutiny: descriptive statistics that summarizes information using statistical parameters; standard deviation, mean, median and inferential statistics that draws conclusions from log data which were subjected to random variation such as sampling variant or observation error that is in-built in the processing software.

CHAPTER FOUR: RESULTS AND DISCUSSION

4.1 Introduction

This chapter describes the interpretation of the radiation log data analysis of the three exploration wells; Kofia-1, Simba-1, Maridadi-1B in Lamu oil exploratory Basin. The results of the wells' petrophysical parameters; lithology (rock type), porosity (ϕ), volume of shale, and fluid saturation are presented in form of tables, plots, and graphs.

In general, the goal of well logging is to ascertain '*zones of interes*t' from a HC buildup perspective by integrating different log response from geophysical tools. The general log response characteristics for HC indications are as follows:

a) Low GR value;

b) Low formation bulk density;

c) Separation of neutron-porosity log combination;

d) High resistivity value;

e) Mud cake formation;

Hence, zones of interest were chosen based on some or all of the above criteria for petrophysical analysis.

4.2 Nuclear data logs and zoning

Zoning is the initial step in any process of nuclear data logs interpretation. During this process the logs (zoning tools) were divided into intervals corresponding to; porous and non-porous formation, clean and shaley rock, good and bad logs based on borehole conditions. In practice, a mature source rock shows high resistivity anomaly, and high GR reading. For a reservoir formation with HC, the readings would show low GR values and relatively high resistivity.

Figure 4.1, 4.2 and 4.3 show the complete nuclear log data (GR, density, neutron), resistivity, and caliper profiles at different depths for the three exploration well; Kofia-1, Maridadi-1B and Simba-1, where the zones of interest corresponding to; low GR, high resistivity, low density are identified.

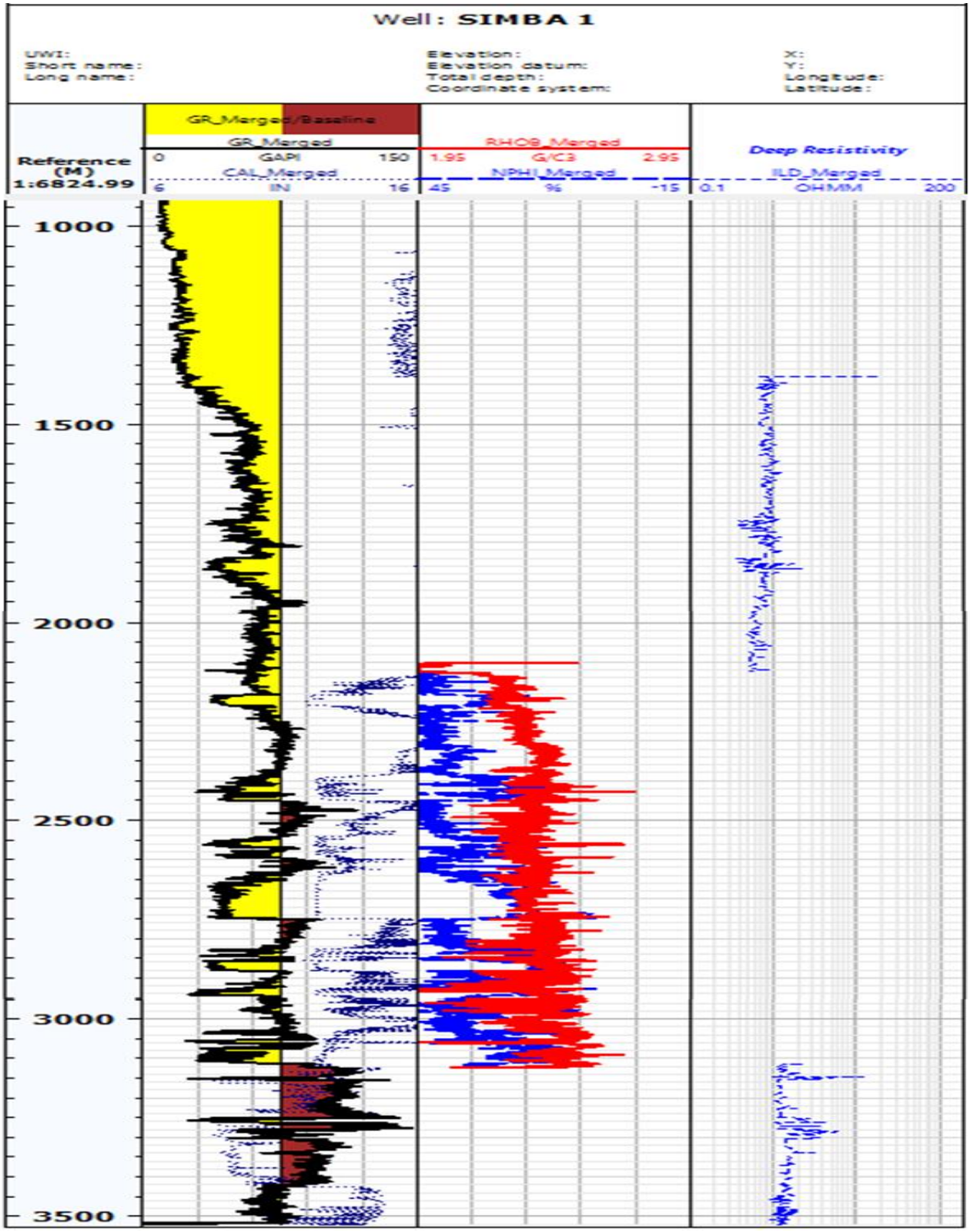

Figure 4.1: Nuclear log data plot for Simba-1

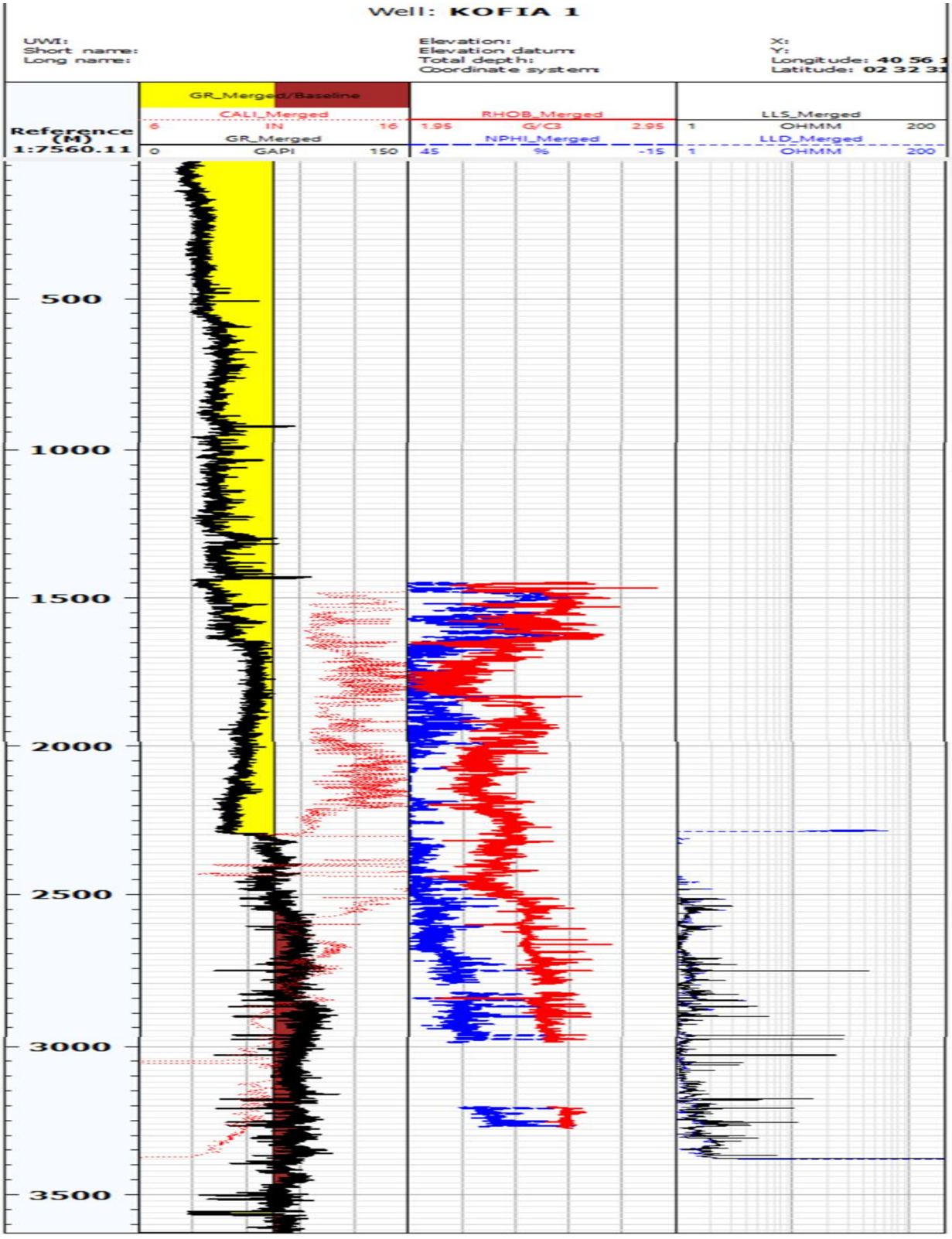

Figure 4.2: Nuclear log data plot for Kofia-1

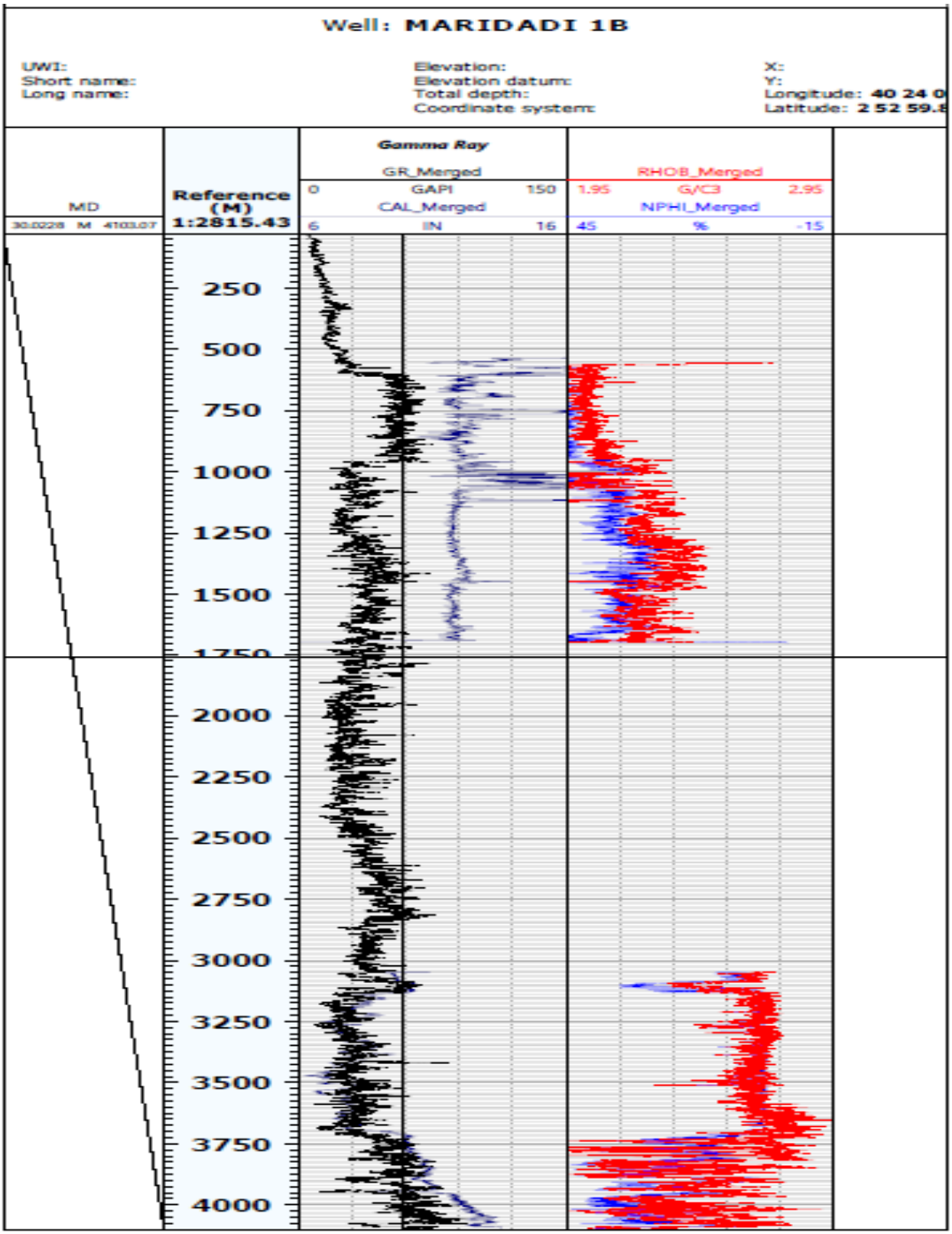

Figure 4.3: Nuclear log data for Maridadi-1B

Figure 4.4, 4.5 and 4.6 show zoomed view of the zones of interest that were identified for Kofia-1, Simba-1 and Maridadi-1B wells. Additional selected zones of interest are found in Appendices D1-D3 at various well depths.

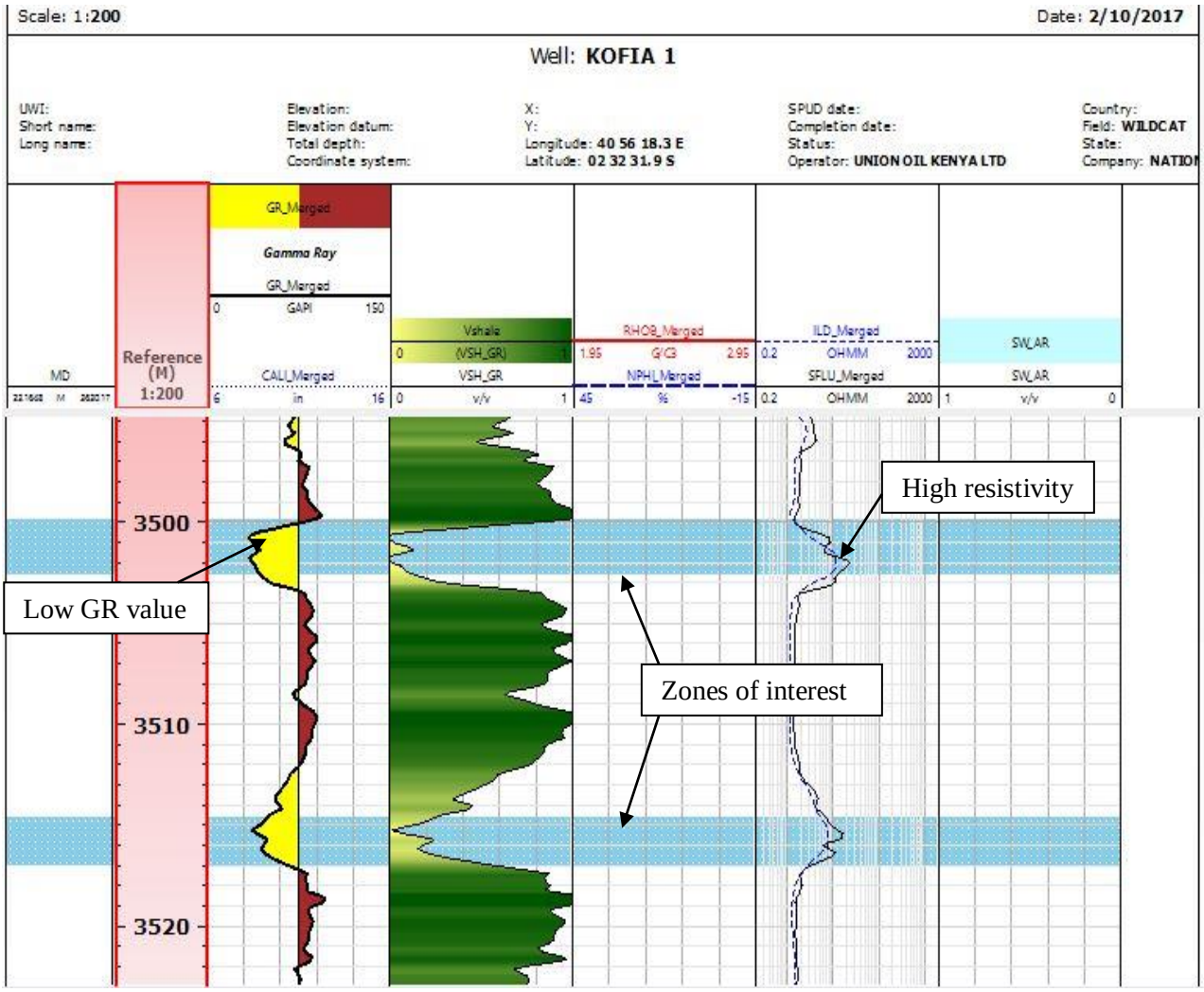

Figure 4.4: Kofia-1 zones of interest.

For lithology determination, baselines for sandstone and shale corresponding to low GR reading and high GR reading respectively are often established on the nuclear log data plots to aid compute V_{sh} and other matrix mineralogy, normally referred to as the sandline and shaleline. Figure 4.4 shows the sand line (33 API) and shale line (90 API) on a gamma log for Kofia-1 well at one of zones. These baselines were used for the quantitative determination of V_{sh} for the given zone.

Figure 4.5 shows the sand line (30 API) and shale line (120 API) on a gamma (GR) log for Simba-1 well at one of zones. These baselines were used for the quantitative determination of V_{sh} for the given zone. Additional selected zones of interest are found in Appendices D1-D3. However, in practice, there could be minor intercalations of siltstone, dolomitic marls, and calcareous shale between the baselines.

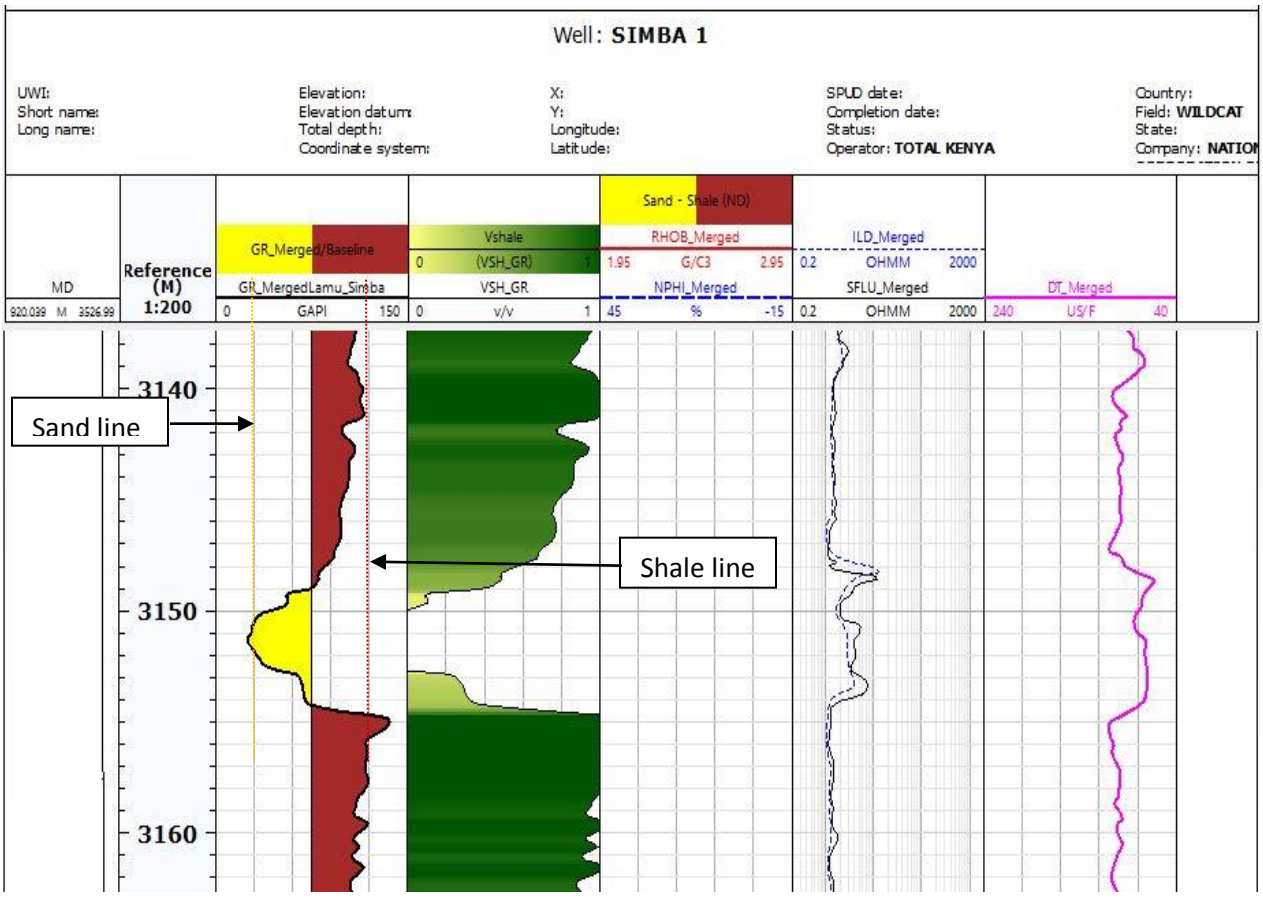

Figure 4.5: Sand line and shale line defined on the GR log in the zone of interest for Simba-1 well

Figure 4.6 shows the available well logs that were used to compute petrophysical parameters within the depth range 2890-3910 meters below sea level. The findings show the calculated S_w (50-80%) and V_{sh} of about 40%-60%). The sand line is at (30 API while the shale line at 75 API on a GR log for Maridadi-1B well at one of zones.

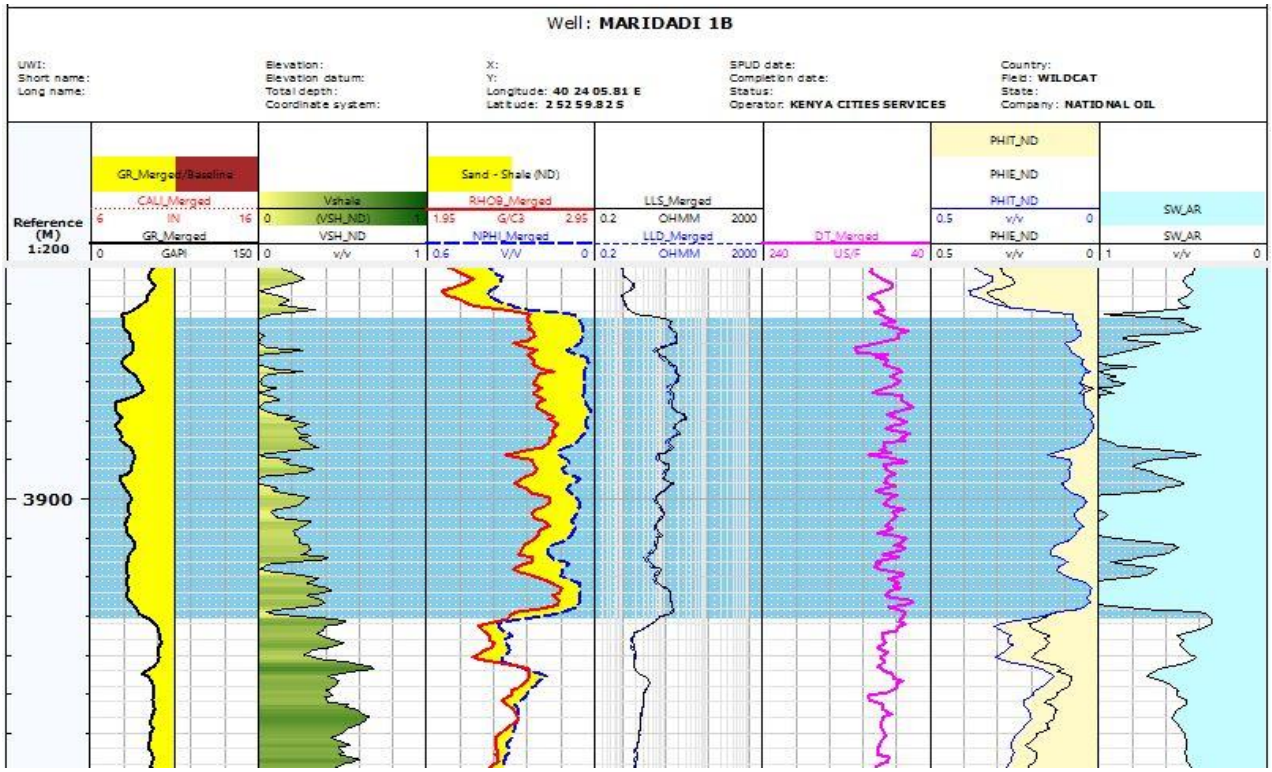

Figure 4.6: Nuclear logs and resultant water saturation at a zone Maridadi-1B well

Table 4.1 is a summary of reservoir zone statistics; formation tops and bottom depths, reservoir thickness for the sample zones of interest were computed for the study wells.

Table 4.1: Well reservoir statistics

WELL RESERVOIR STATISTICS						
Wells	**Formation Top (m)**	**Formation Bottom (m)**	**Gross Reservoir(m)**	**Net Reservoir (m)**	**Net/Gross**	**Expected Hydrocarbon**
Kofia-1	3500	3570	70	11	0.16	Oil/Gas shows
Maridadi-1B	3150	3950	800	162	0.20	Oil/Gas shows
Simba-1	2600	2750	150	30	0.20	
	3250	3310	60	10	0.17	Gas shows

Table 4.1 above shows that the three wells under investigation have a net-gross ratio of 0.16 - 0.2, implying that approximately 20% of their formation is sandstone. This is an indication of poor reservoir quality for possible gas/oil shows. A good reservoir quality would have more than 50% net-gross ratio (Nyaga, 1995).

Nevertheless, data from the three wells were analyzed for distribution of petrophysical parameters; water saturation, porosity, permeability, and reservoir thickness was determined based on well log data, in addition.

4.3 Determination of petrophysical parameters

4.3.1 Petrophysical parameters Kofia-1

Table 4.2 is a summary of results of petrophysical parameters in kofia-1

Table 4.2: Results of petrophysical parameters for Kofia-1

Zone	Depth (m)	Reservoir thickness (m)	Por (%)	S_w (%)	V_{sh} GR (%)	HC predicted
1	3500-3504	3	20	38	16	Gas
2	3514-3518	3	22	39	20	Gas
3	3556-3559	2	28	33	10	Oil
4	3564-3569	3	31	32	10	Oil

For Kofia-1 well, a total of four (4) hydrocarbon (HC) bearing zones were demarcated with a pay zone of 11 m as shown in table 4.2. The estimated porosity values for the oil zones (28% - 31%) were higher than the gas zones (19%-22%). The water saturation (S_w) range varied between 32%-39%, in all zones identified, implying that more than 60% of the reservoir could be filled with hydrocarbon. The S_w values were determined based on resistivity measurements from well head reports, of approximately 87 Ω.m, while that of mud fluid was 0.6 Ω.m for Kofia-1 Well. However, the total pay zone suggests a reservoir potential that is insufficient for exploitation. Figure 4.7 shows the computed water saturation profiles for Kofia-1 and an estimated clean zone of 40 API and the shale zone of 105 API.

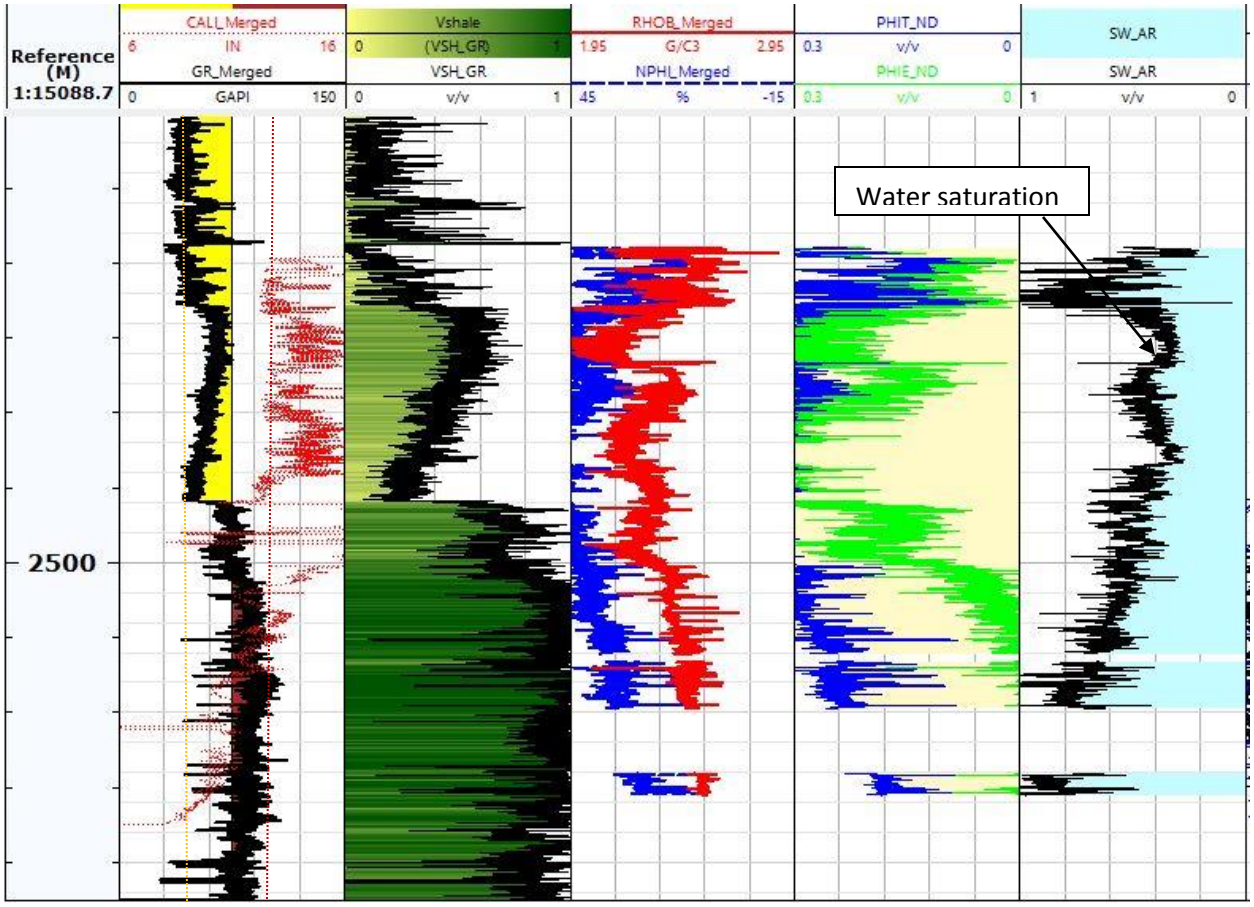

Figure 4.7: Water saturation profiles in Kofia-1 well

4.3.2 Petrophysical parameters Maridadi-1B

Table 4.3 is a summary of results of petrophysical parameters in Maridadi-1B

Table 4.3: Results for petrophysical parameters of Maridadi-1B

Zone	Depth (m)	Reservoir thickness (m)	Por (%)	S_w (%)	V_{sh} GR (%)	HC predicted
1	3150-3154	2	27	66	16	Gas
2	3420-3425	4	31	54	23	Gas
3	3934-3940	3	35	60	16	Oil

The three delineated zones exhibited two for gas and one for oil, with a pay zone of about 9 m are identified in Maridadi-1B. . The estimated porosity values for the oil zone (35%) were higher

than the gas zones (27%-31%). The water saturation (S_w) range varied between 54%-66%, in all zones identified. The resistivity measurements from well head reports, was 150 Ω.m. However, the total well pay zone suggests a reservoir potential that is insufficient for exploitation. The GR log estimation form Maridadi-1B gives a clean zone of 30 API while the shale zone starts at 75 API.

Figure 4.8 shows the computed water saturation profiles for Maridadi-1B. In general, the high water saturation indicates low hydrocarbon content, the overlapping neutron-density crossplot points to presence of limestone in the wellbore.

Drill cuttings from Maridadi-1B exploration well have been interpreted previously to indicate presence of oil in gas or water saturated reservoir (Nyaga, 1995). This points to the presence of oil derived from Upper cretaceous or even young calcareous rock, contrary to the belief that viable source rocks can only be from Jurassic or older lithologies.

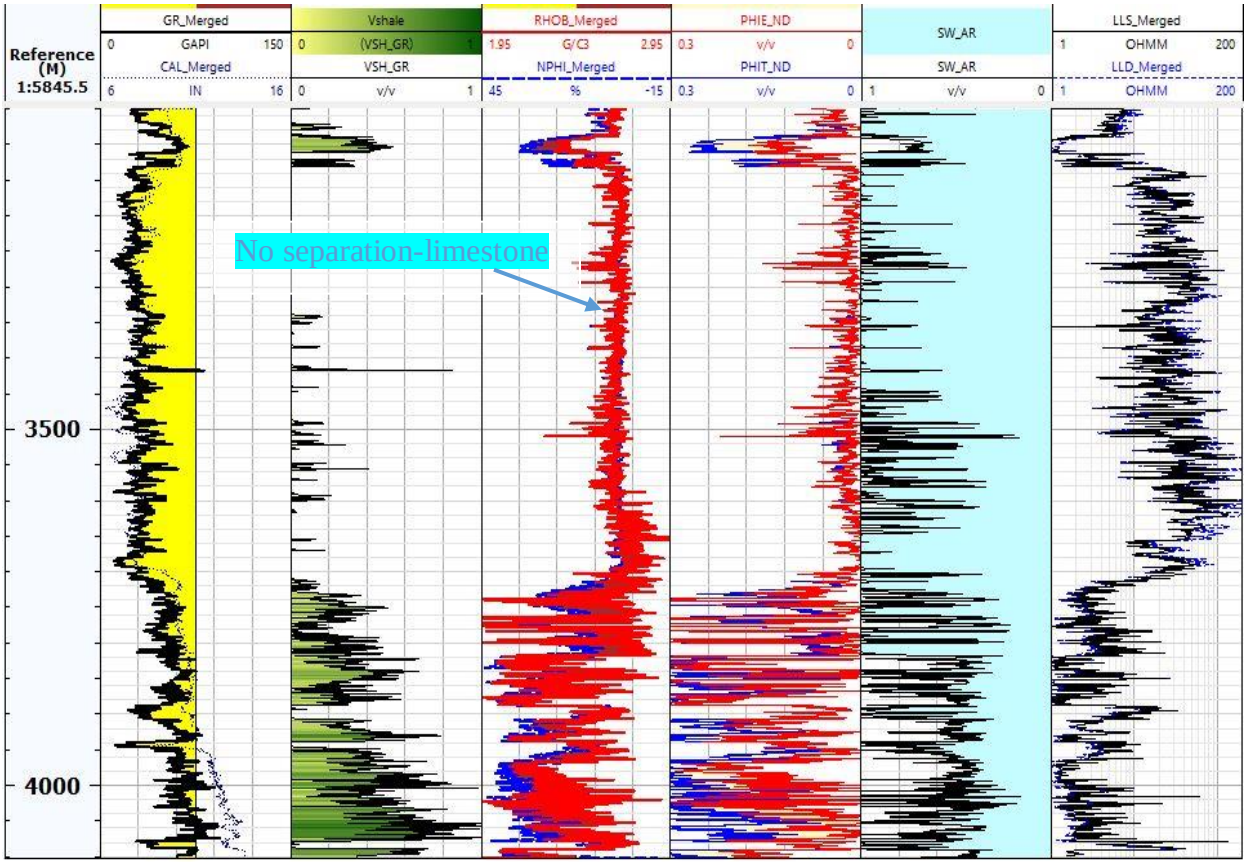

Figure 4.8: Water saturation in Maridadi-1B well in limestone formation

4.3.3 Petrophysical parameters for Simba-1

Table 4.4 shows the results of petrophysical parameters for Simba-1well

Table 4.4: Results of petrophysical parameters for Simba-1

Zone	Depth (m)	Reservoir thick..(m)	Por (%)	S_w (%)	V_{sh} GR (%)	HC predicted
1	3119-3123	3	31	66	16	Gas
2	3147-3150	2	35	57	21	Oil
3	3255-3262	6	37	63	17	Oil

The GR log for Simba-1 well gives an estimation of the clean zone at 35 API and the shale zone at 110 API. The formation resistivity in the zone of interest is approximately 104 Ω.m, and mud fluid resistivity of 0.52 Ω.m, while water saturation was approximately between 57% - 66%.

Three (3) HC bearing zones were delineated at separate intervals between 3119 m – 3262 m. Figures 4.9 shows the computed water saturation profiles for Simba-1. In general, the high water saturation indicates low hydrocarbon content, while the large positive separation in neutron-porosity crossplot indicates shale in the wellbore.

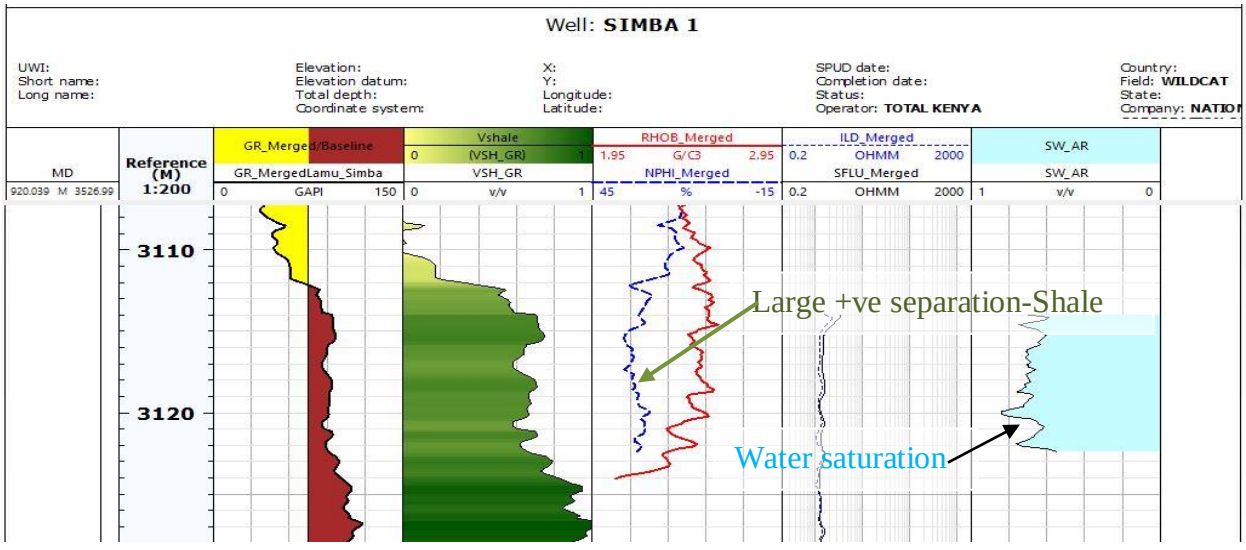

Figure 4.9: Water saturation in Simba-1 well

4.3.4 Density-Neutron cross-plots : Lithology identification

Figure 4.10 shows the results of computed petrophysical parameters within the depth range 3936-3955 meters below sea level. The findings show shale and sandstone formations, S_w (35-70%), porosity of 29%, and V_{sh} of average of about 20%.

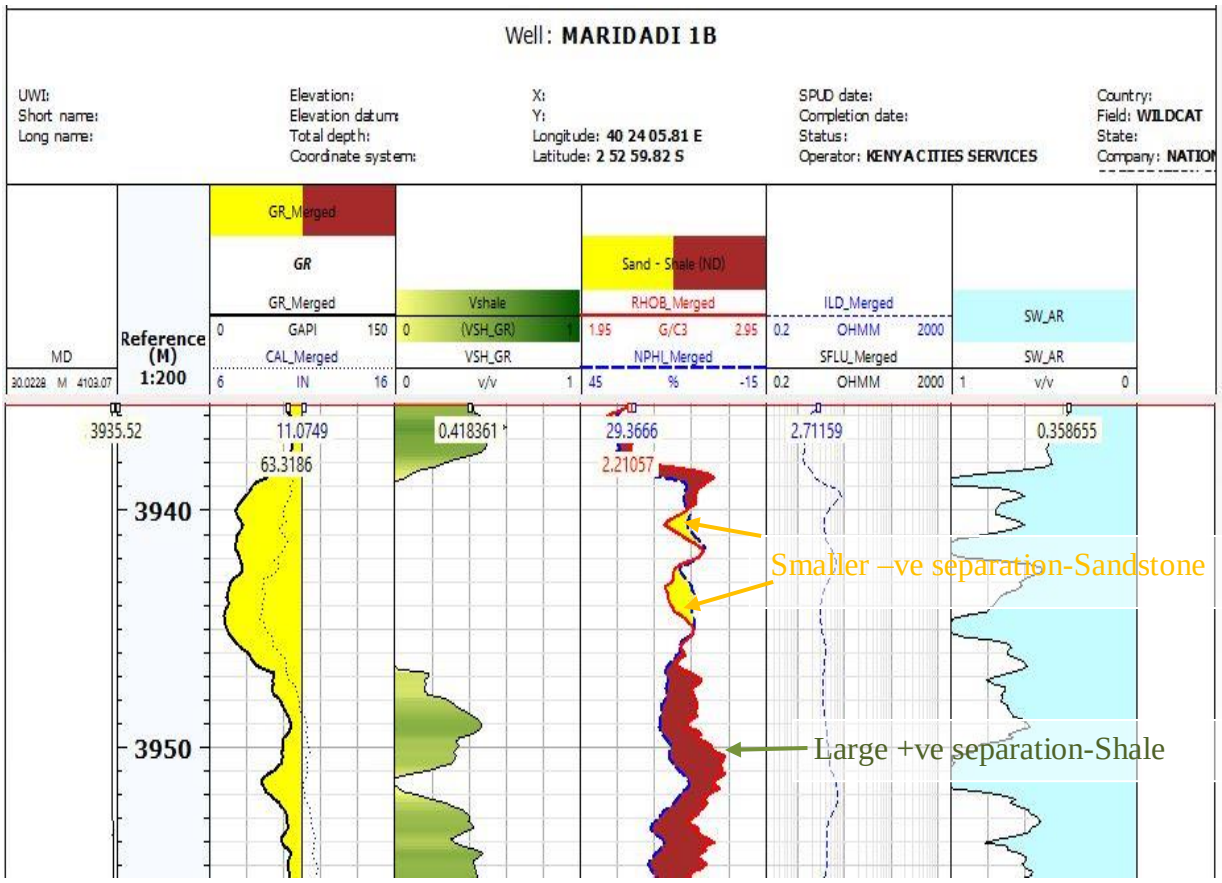

Figure 4.10: Lithology identification from neutron-density log combination-crossover

The different porosity logs respond differently to fluid and mineral combinations. Therefore, the neutron-density cross-plot or other different porosity logs can be utilized to identify lithology/mineral proportions and corroborate individual nuclear log data. Figure 4.11a and b shows the density-neutron cross-plot used to determine lithology or V_{sh}, and porosity in Maridadi-1B well. The cross-plot of well strata depth, shows range between 1000-3000 m below sea level, shows that limestone is the dominant lithology in Maridadi-1B well , based on the low gamma reading (30-40 API) on the GR scale in Figure 4.8a.

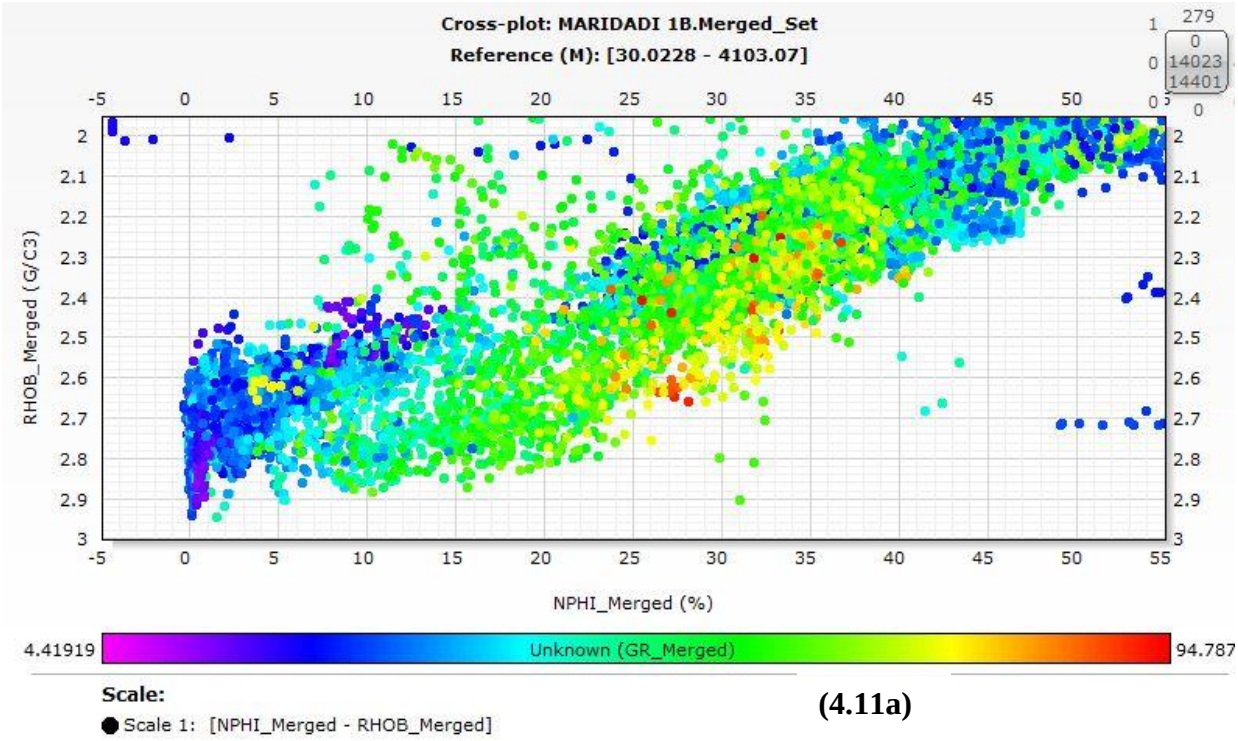

(4.11a)

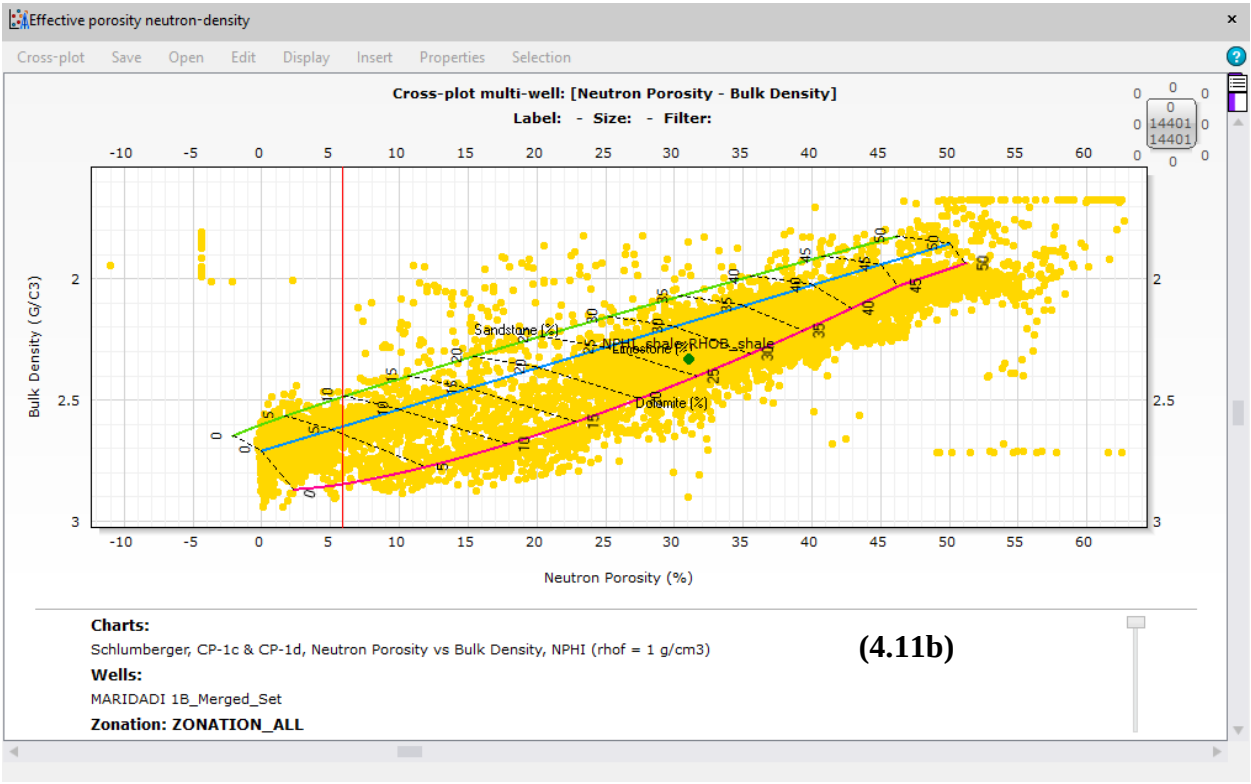

(4.11b)

Figure 4.11: a) Density-Porosity cross-plot on GR scale b) lithology determination in Maridadi-1B

This result is further corroborated by Figure 4.11b plots, which shows limestone is dominant (blue line) with interspersed with a few sandstone (green line) and dolomite (red line) indications. This finding confirms the earlier results obtained using nuclear log profiles in section 4.3.2.

Lithology for the wellbore was achieved after zooming in on the respective log tracks to gain finer details for profile. The same procedure is repeated for all the three wells under consideration. The general stratigraphic profile for the wells is presented in Appendices D4-D6 showing resultant lithology profiles for the wells under study. Simba-1 wellbore is dominated with shale and a sandstone rock, Kofi-1 has shales, limestone and dolomite, while Maridadi-1B well consists of limestone, shale and sandstone formations.

4.3.5 Determination of Permeability

Permeability was computed from porosity values at the zones of interest using the formulas in section 3.2.4. The resultant permeability was determined using the porosity range values between 20%-37% in the three wells between 21 mD and 116 mD for oil reservoir.

Research conducted in east Africa and offshore basins around the world where petroleum has been discovered show relatively similar results for petrophysical parameters except the hydrocarbon saturation. There is limited information previously conducted on petrophysical data for the specific wells studied in offshore Lamu Basin. However, there is regional data in existence. For example, oil exploration in the southern coast of Tanzania gave values of porosity at 14-20%, permeability of 4mD-14mD, and S_w of about 70% (Lyaka and Mulibo, 2018). Despite good porosity and the low *K*, high S_w led to the conclusion that the east Pande project was a poor prospect.

In Mozambique, porosity of 25-30% and S_w of 50-65% have been reported in current economical gas reservoirs (Mashaba and Altermann, 2015). In this study, our petrophysical parameters values are closer to those reported in the oil rich onshore Niger basin by Opara (2010).

CHAPTER FIVE: CONCLUSIONS AND RECOMMENDATIONS

5.1 Introduction

The objective of this project was to use nuclear well log data to estimate petrophysical parameters in order to characterize the hydrocarbon potential of offshore Lamu Basin. On account of the outcomes of the study and the available data, conclusions and recommendations are made in subsequent subsections.

5.2 Conclusion

Log analysis techniques were successfully applied to nuclear well log data from three exploration wells in the offshore Lamu Basin. Composite logs of the three wells studied, indicate that all the reservoir formations drilled occurred in the local geology consisting of shale, limestone and sandstone of the Karoo. The results of petrophysical parameters; porosity, water saturation, permeability, volume of shale, and pay zone (reservoir thickness) were applied to illustrate the reservoir prospective of the Lamu basin. The resultant distribution of the preceding petrophysical parameters based on nuclear log interpretation made it possible to draw the below conclusions:

a) The zones of interest for oil and gas in the three exploration wells ranged between 2600 m and 3900 m below mean sea level;

b) Porosity at the zones of interest for the three wells studied is placed at 28±7%;

c) Water saturation in the zones of interest is 45±15%;

d) The volume of shale (Vsh) is low, 20±4% in projected reservoir zones;

e) Permeability derived from porosity values ranges between 21mD and 116mD;

f) Hydrocarbon pay zones ranged between 3m to 11m;

g) Lamu basin has potential for hydrocarbons; however the quantity in the studied wells is undeterminable due to lack of delineated area from seismic.

The results show delineated oil bearing zones as being more porous than their gas bearing counterparts, which in theory is in order, as gas , normally has less hydrogen concentration that fluctuates with pressure and temperature. Consequently, when gas occurs within the wellbore zone of investigation, the formation density log shows high porosity, while neutron log depicts an under-estimated porosity. The estimated hydrocarbon pay zones of 3-11 m are indication low potential for oil and gas accumulation in the wells.

The reservoir quality within the offshore Lamu basin is affected by several faults with different throws, which tend to be sealing resulting in areal compartments. Therefore some form of reservoir simulation approach is advised to determine the dominant flow direction of fluids in the basin. The radiation log techniques used, are cost effective, in determining petrophysical parameters for hydrocarbon prospecting.

5.2 Recommendations

1) To drill horizontal directional wells to overcome the issue of compartmentalization in the formation. In practice, horizontal wells allow connection of the fault blocks for increased reservoir pay zone.

2) To use NMR log data in future exploratory wells – which is effective for determining permeability in complex lithology?

3) To use seismic data to determine reservoir spatial distribution (area) for computation of the quantity of hydrocarbons in basin.

List of References

Abouzaid, A., Thern, H., Said, M., ElSaqqa, M., Elbastawesy, M., & Ghozlan, S. (2016). Nuclear Magnetic Resonance Logging While Drilling in Complex Lithology - Solution for a Glauconitic Sandstone Reservoir. *Society of Petroleum Engineers*

Allaud, L.A, & Martin, M.H. (1977). Schlumberger: The history of well log technique. John Wiley and sons Inc.

AlRuwaili, S. B. (2005). Frontiers of Formation Evaluation and Petrophysics; Present and Future Technologies. *Society of Petroleum Engineers.* doi:10.2118/106335-MS

Archie, G. E. (1942). The electrical resistivity log as an aid in determining some reservoir characteristics: *Petroleum Technology*, V.S, p.54-62.

Asquith,G. (1985). Handbook of Log Evaluation Techniques for Carbonate Reservoirs. Methods in Exploration Series #5, *AAPG*

Assaad F.A. & LaMoreaux P.E. (2004). Geophysical Well Logging Methods and Interpretations. In: Hughes T.H. (eds) Field Methods for Geologists and Hydrogeologists. Springer, Berlin, p.151-173

Axelrod, M. C., & Hearst, J. R. (1984). Calibration of a Neutron Log in Partially Saturated Media IV: Effects of Sonde-Wall Gap", *SPWLA*, Paper Q.

Baker, R. O., Yarranton, H. W., & Jensen, J. (2015). Practical reservoir engineering and characterization. Elsevier BV

Baker-Hughes-Atlas. (2002). Introduction to Wireline Logging, Ed. Bigelow

Bassiouni, Z. (1994). Theory, Measurements and interpretation of Well logs, *Society Petroleum Engineering* Vol.4 Textbook Series

Bloch, S. (1993). Empirical Prediction of Porosity and Permeability *AAPG* Bulletin 77

Bosworth, W., & Morley, C.K. (1994). Structural and stratigraphic evolution of the Anza rift, Kenya. *Tectonophysics* vol. 236 issue 1-4. p. 93-115

Crain E. R. (1986). The Log Analysis Handbook. Pennwell, Publishing Company Tulsa, Oklahoma, USA.

Cruciani F., Barchi M., Koy H., & Porreca M. (2017). Kinematic evolution of a regional-scale gravity-driven deepwater fold-and-thrust belt: The Lamu Basin case-history (East Africa). *Tectonophysics,* 712–713, 30–44, http://dx.doi.org/10.1016/j.tecto.2017.05.002

Desbrandes, R. (1985). Encyclopedia of well logging: Graham & Trotman, London, p.584.

Donaldson, A., & Clydesdale, G. M. (1990). "Accurate reservoir evaluation quality core samples—a good starting point," in P. F. Worthington, ed., Advances in core evaluation: Gordon and Breach, New York, p. 35-53.

Doveton, J. H. (1994). Geological Log Analysis Using Computer Methods. *AAPG* Computer Applications in Geology, No. 2, *AAPG*, Tulsa, pp.169.

Dunn, K.J., Bergman, D.J., & La Torraca G.A. (2002). Nuclear Magnetic Resonance: Petrophysical and Logging Applications. *Handbook of geophysical Exploration: Seismic Exploration* Vol 32, Pergamon, New York

Durrance, E.M. (1986). Radioactivity in Geology: Principals and Applications. John Wiley

Eames, F. E. & Kent P. E. (1955). Miocene Beds of the East African Coast. *Geological Magazine* 92(04):338 - 344.

Edmundson, H. & Raymer, L. (1979). Radioactive Logging Parameters for Common Minerals, *SPWLA* Trans., June 3-6.

Ellis, D. V., & Singer, J. M. (2008). Well logging for earth scientists. Dordrecht: Springer.

Farag, M. I. A.-F. I. (2010). Geophysical reservoir evaluation of Obaiyed Field, western desert, Egypt.

Gaymard, R. & Poupon, A. (1968). Response of Neutron and Formation Density Logs in Hydrocarbon Formations. *The Log Analyst, September-October*

Harvey P.K. & Lovell, M.A. (1998). Core-Log Integration, *Geological Society Pub*. 136,

Heart, J., Nelson, P., & Paillet, F. (2000). Well Logging for Physical Properties: A Handbook for Geophysicists, Geologists, and Engineers, 2nd Edition, Wiley

Helander, D. (1983). Fundamentals of formation Evaluation, OGCI

Heya, M. (2012). *Petroleum Exploration Overview in Kenya*, Presentation at the 19th Engineers International Conference. Ministry of Energy, Kenya, (accessed 12th January, 2016).

Jackson, J.A. (2001). The history of NMR well logging, publishers: John Wiley $ Sons Inc.

Johnson, H.M. (1962). A history of well logging, *SEG Geophysics*, Volume 27, p 507.

Kerr, J. W., MacKeith, N. W., Nyagah, K., & Ngenoh, D. K. (1996). Hydrocarbon Potential of the Basins of Kenya. AAPG

Kozhevnikov, D., Kovalenko, K., & Deshenenkov, I. S. (2011). Informational Advantages and Accuracy Characteristics of the Adaptive Well Log Data Interpretation. Society of Petroleum Engineers. doi:10.2118/148676-MS

Krygowski, D. & Asquith, G. (2005). Basic Well Log Analysis. *AAPG*

Liu, H. (2017). Principles and Applications of Well Logging, 2nd Edition. Springer-Verlag Berlin Heidelberg. Springer Nature

Lyaka, A.L. and Mulibo, G.D. (2018) Petrophysical Analysis of the Mpapai Well Logs in the East Pande Exploration Block, Southern Coast of Tanzania: Geological Implication on the Hydrocarbon Potential. Open Journal of Geology, 8, 781-802.

Martin, F. D. & Colpitts R.M. (1996). Reservoir Engineering. In: Lyons W.C. (eds) Stanadarad Handbook of Petroleum and Natural Gas Engineering. Elsevier Science, Vol 2, p. 1-362

Mashaba, V. and Altermann, W. (2015). Calculation of water saturation in low resistivity gas reservoirs and pay-zones of the Cretaceous Grudja Formation, onshore Mozambique basin. *Marine and Petroleum Geology*, 67, pp.249-261

Masinde, A. (2015). Structural evolution of the Simba high offshore Kenya, and its implications for hydrocarbon potential. *Unpublished Thesis University of Leeds.*

Mbede, E.I., & Dualeh, A. (1997). The Coastal Basins of Somalia, Kenya and Tanzania. From African Basins, *in* R.C. Selley (ed) African Basins, Sedimentary Basins of the World 3, *Elsevier Science*, p. 212-234.

Mheluka, J. & Mulibo, G. (2018). Petrophysical Analysis of the Mpera Well in the Exploration Block 7, Offshore Tanzania: Implication on Hydrocarbon Reservoir Rock Potential. *Open Journal of Geology*, **8**, 803-818. doi: 10.4236/ojg.2018.88047.

Nelson, R. J., & Mitchell, W. K. (1991). Improved Vertical Resolution of Well Logs by Resolution Matching. *The Log Analyst, Vol. 32, No. 4, July-August.*

NOCK. (1995). Hydrocarbon Potential of the Coastal Onshore and Offshore Lamu Basin of South-East Kenya: Integrated Report and Enclosures. *Unpublished*

Nyagah, K. (1995). Stratigraphy, depositional history and environments of deposition of Cretaceous through Tertiary strata in the Lamu Basin, southeast Kenya and implications for reservoirs for hydrocarbon exploration. *Sedimentary Geology* vol. 96 (1-2), p. 43-71

Okechukwu, E. A., Igboekwe, M., Chukwu, G., & Etuk, S. E. (2018). Discrimination of Pore Fluid and Lithology of a Well in X Field, Niger Delta. *Arabian Journal of Geoscienc*.

Opara A.I. (2010). Prospectivity evaluation of ‘‘Usso Field’’, onshore Niger Delta basin using 3-D seismic and well log data. Petrol Coal 52(4):307–315

Osicki, O., Schenk, O. & Kornpihl, D. (2015). Prospectivity and Petroleum Systems Modelling of the Offshore Lamu Basin, Kenya: Implications for an Emerging Hydrocarbon Province. *AAPG*.

Podgorsak, E.B. (2005). Radiation Oncology Physics: A Handbook For Teachers And Students. International Atomic Energy Agency.

Pugh, V. J., Thomas, D. C., & Gupta, S. P. (1991). Correlations of liquid and air permeabilities for use in reservoir engineering studies: *The Log Analyst*, v. 32, no. 5, p. 493-497.

Ransom, R.C. (1977). Methods based on density and neutron well logging responses to distinguish characteristics of shaly sandstone reservoir rock: *Log Analyst*, v.18, p. 47-63.

Rider, M. H. (2002). The geological interpretation of well logs 2nd ed., rev. Sutherland: Rider-French Consulting.

Sagesman, F.F. (1980). Well logging method, Geophysics, 45, p 1667-1668.

Schlumberger Ltd. (1987). Log Interpretation Charts," Houston, Texas,

Schlumberger Ltd. (1989). Log Interpretation Principles/Applications, Well Services, Houston.

Tiab, D. & Donaldson, E. C. (2004). Petrophysics: Theory and Practice of Measuring Reservoir Fluid Properties. 2nd Ed. New York: Elsevier

Wyllie, M.R.J. & Rose, W.D. (1950). Some Theoretical Considerations Related to the Quantitative Evaluation of the Physical Characteristics of Reservoir Rock from Electric Log Data, *Trans., AIME*, Vol. 189, pp. 105.

Yang, Z. & Hirasaki, G. (2008). NMR measurement of bitumen at different temperatures. *Journal of magnetic resonance*

Zhao, P., Mao, Z., Jin, D., Zhao, P., Sun, B., Sun, W., & Pang, X. (2015). Investigation on log responses of bulk density and thermal neutrons in coalbed with different ranks, *Journal of Geophysics and Engineering*, Volume 12, Issue 3, pp. 477–484.

Zongying, Z., Ye T., Shujun, L. & Wenlong, D. (2013). Hydrocarbon potential in the key basins in the East Coast of Africa. *Petroleum Exploration and Development*, 40, p.582-591.

Appendices

A. Location, general geology and well Schematics

A.1. Kenyan map showing results of drilled exploration wells in various basins by 2015

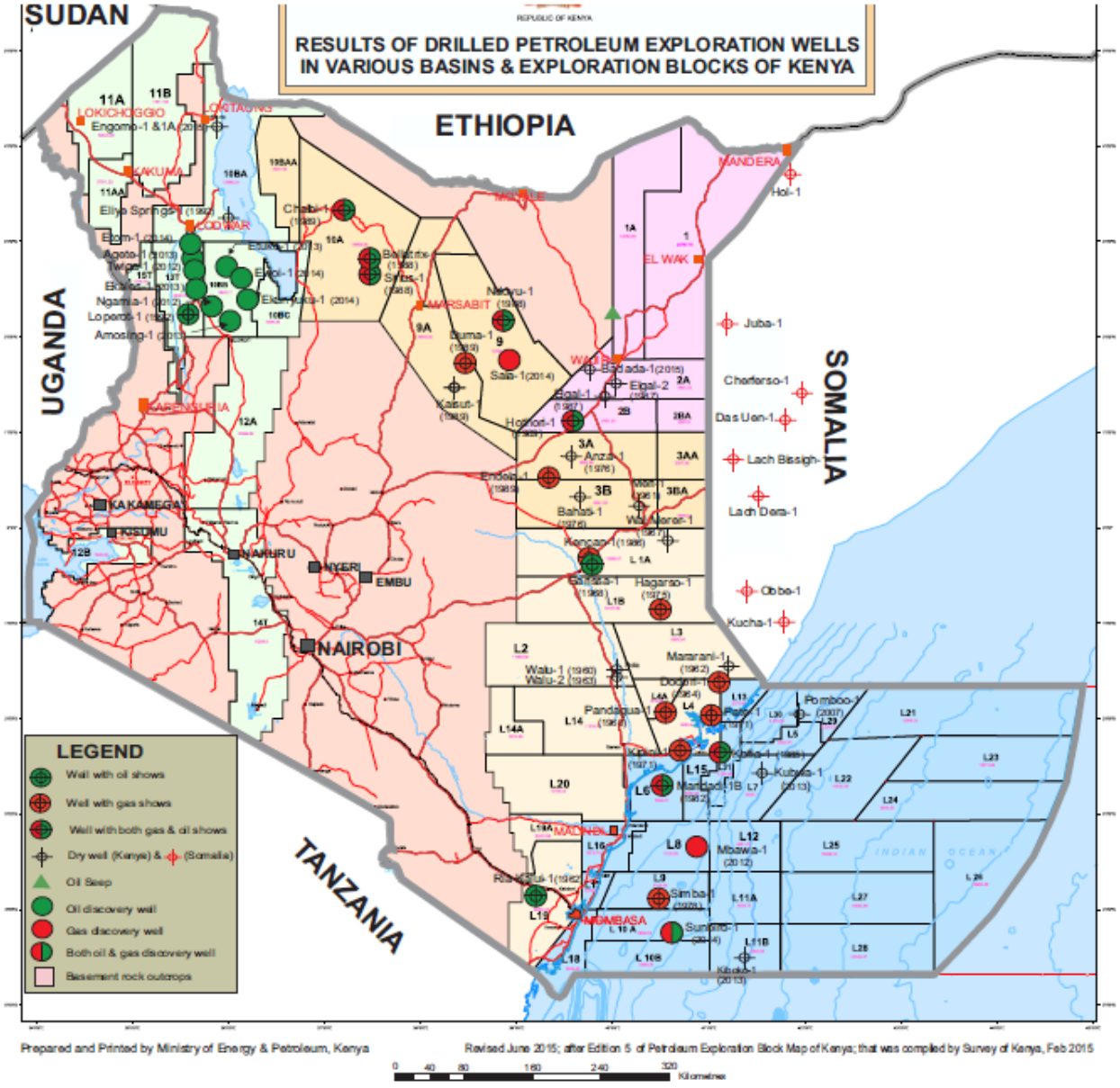

A.2. Stratigraphy of lithologies in the passive margin of Lamu basin (Zongying et al., 2013)

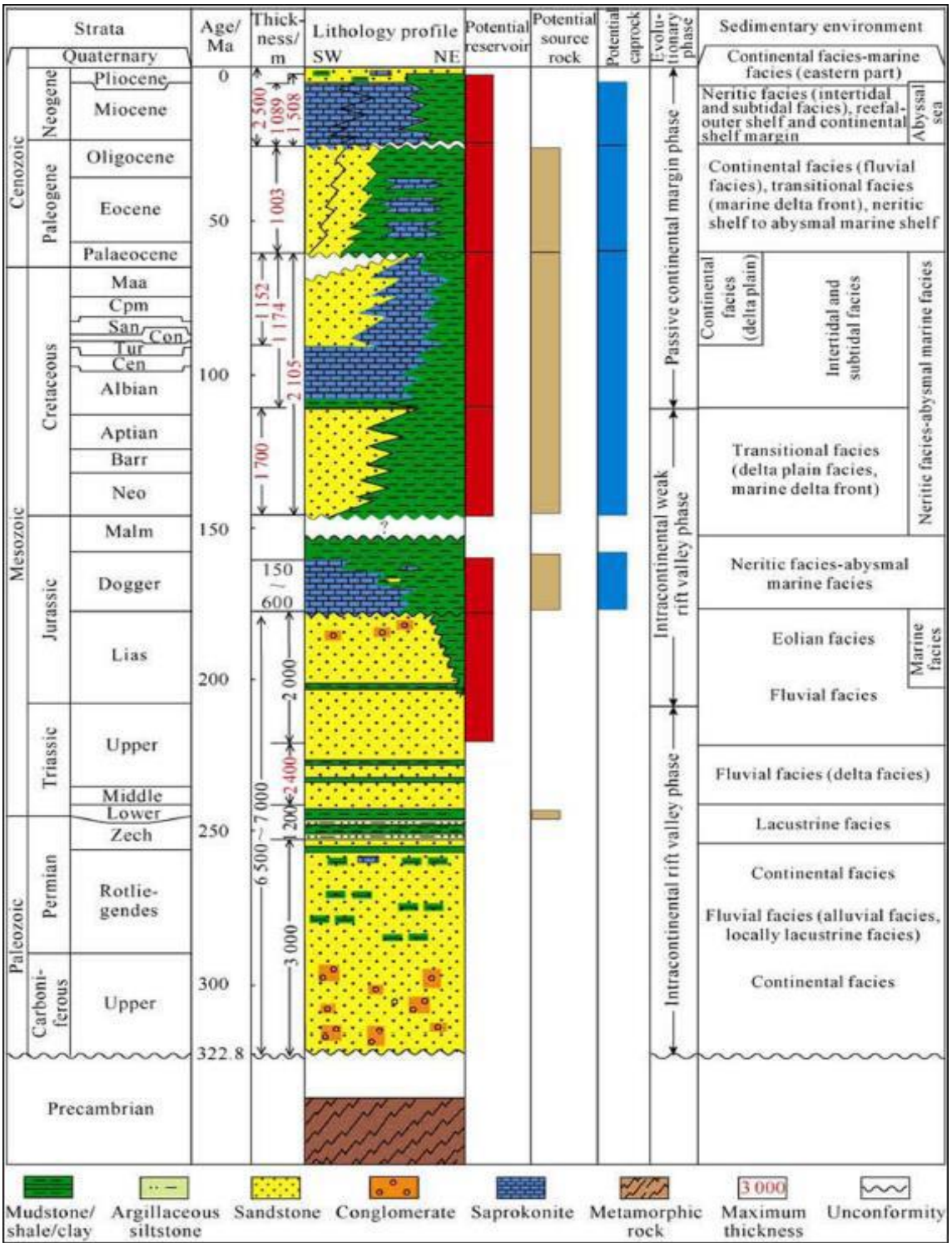

B: Tools and Equipment

B.1. Well logging tools: lengths range 10-20m; diameters ~3 inches

After Ellis and Singer, 2008

C. Well geometry schematics

C.1. Simba-1 well schematic drilling presentation

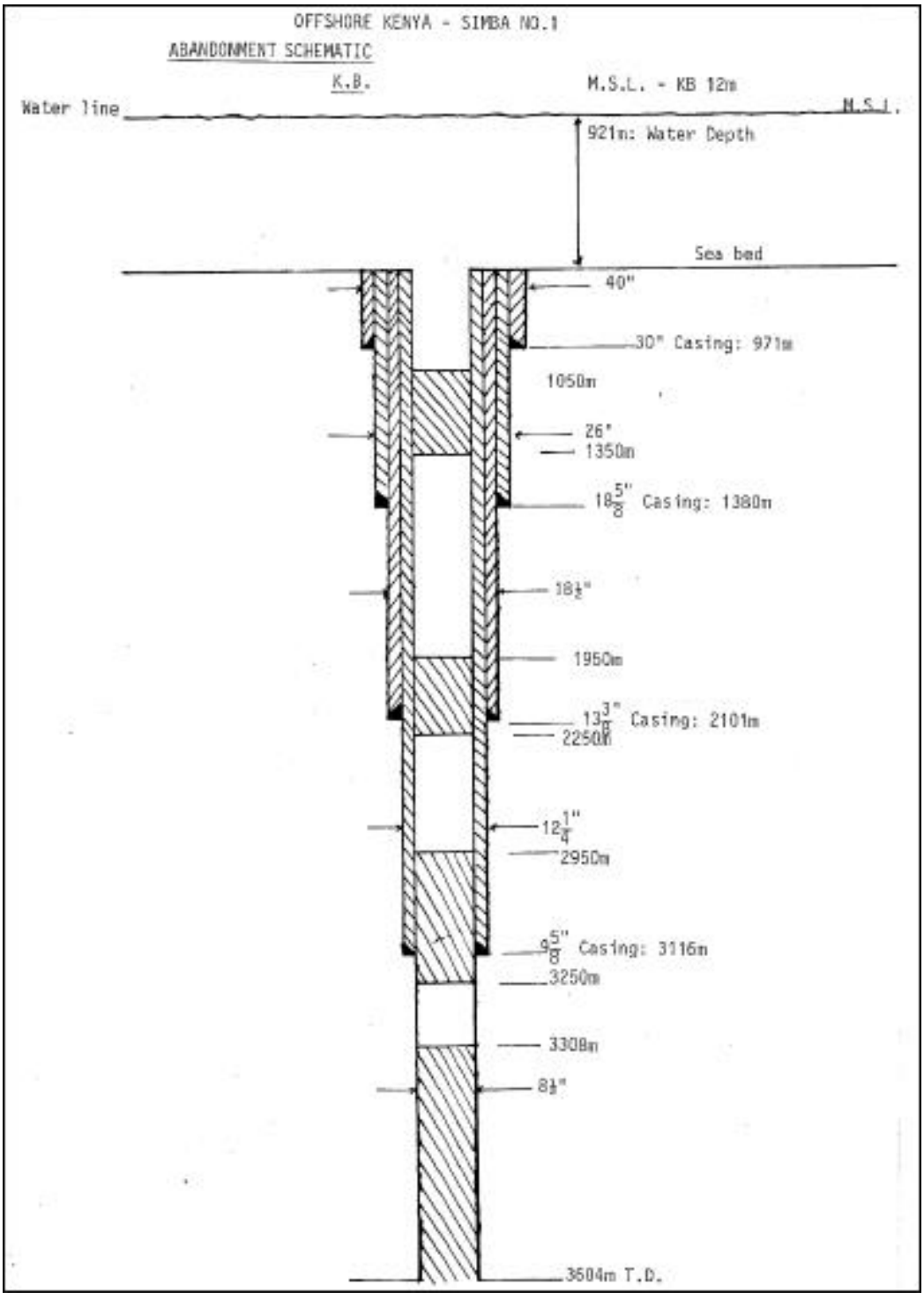

C.2. Maridadi-1B well schematic presentation

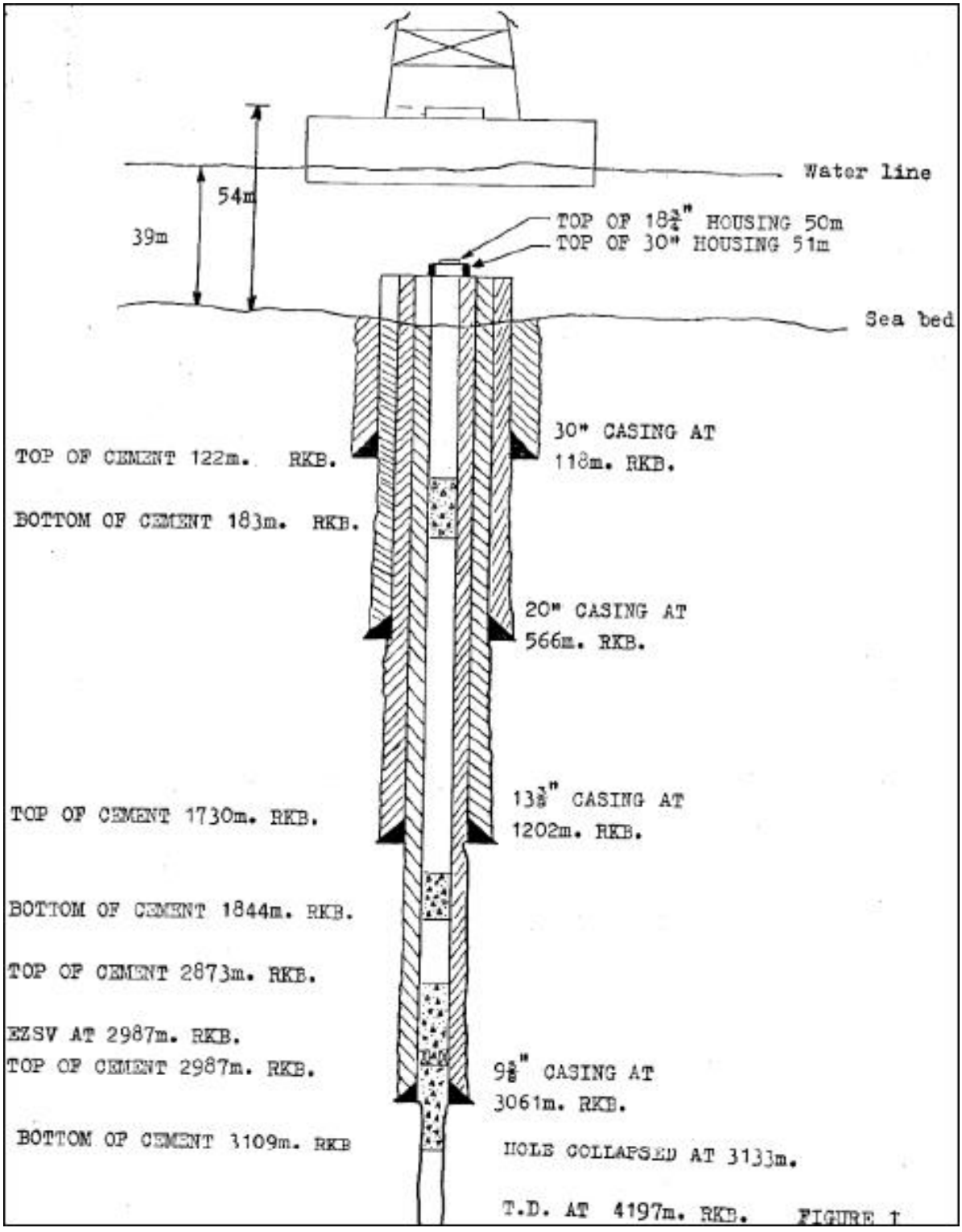

C.3. Kofia-1 well schematic drilling and geological log

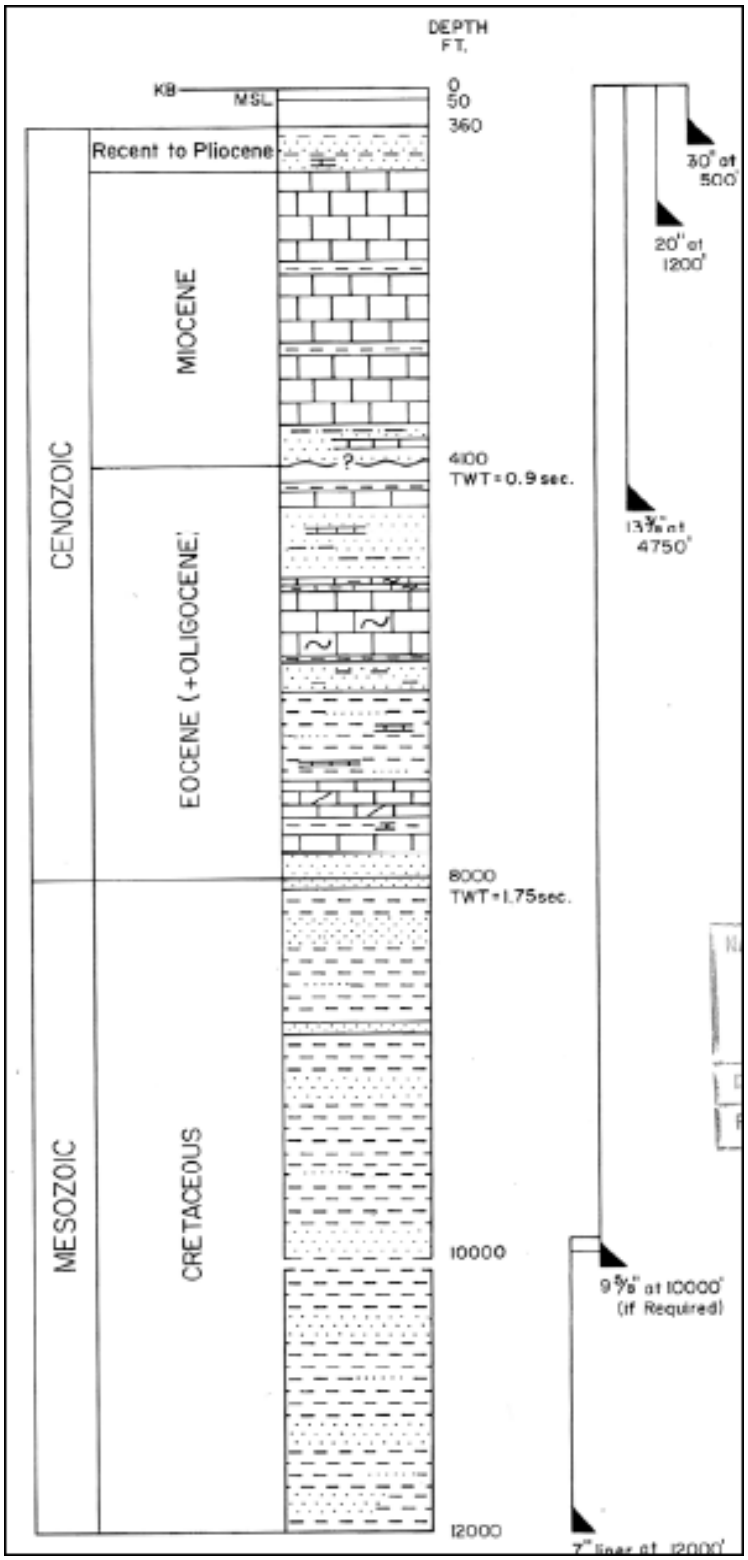

C.4. Sample Simba-1 well data in compatible LAS format.

```
~Version
 VERS                .          3.0                            : CWLS LOG ASCII STANDARD - VERSION 3.0
 WRAP                .          NO                             : ONE LINE PER DEPTH STEP
 DLM                 .          SPACE                          : DELIMITING CHARACTER(SPACE TAB OR COMMA)
~Well Information
#_____________________________________________________________________________
#
#PARAMETER_NAME     .UNIT      VALUE                          : DESCRIPTION
#_____________________________________________________________________________
STRT                .M         920.0388                       : First reference value
STOP                .M         3526.9932                      : Last reference value
STEP                .M         0.1524                         : Step increment
NULL                .          -9999                          : Missing value
COMP                .          NATIONAL OIL CORPORATION OF KENYA LTD: Company
WELL                .          SIMBA 1                        : Well name
FLD                 .          WILDCAT                        : Field
LOC                 .          X 40 34 0896  Y 04 00 2761     : Location
SRVC                .          Schlumberger                   : Service Company
CTRY                .                                         : Country
DATE                .                                         : Service Date
LATI                .                                         : Latitude
LONG                .                                         : Longitude
GDAT                .                                         : Geodetic Datum

#LOGNAME            .UNIT      LOG_ID                         : DESCRIPTION
#_____________________________________________________________________________
MD                  .M                                        :  {F}
CAL_Merged          .IN                                       :  {F}
DRHO_Merged         .G/C3                                     :  {F}
DT_Merged           .US/F                                     :  {F}
GR_Merged           .GAPI                                     :  {F}
ILD_Merged          .OHMM                                     :  {F}
NPHI_Merged         .%                                        :  {F}
RHOB_Merged         .G/C3                                     :  {F}
SFLU_Merged         .OHMM                                     :  {F}
SP_Merged           .mV                                       :  {F}
~Ascii
920.0388   18.60397   -9999      -9999      8.956370353698731 -9999      -9999      -9999      -9999      -9999
920.1912   18.06084   -9999      -9999      9.270520210266112 -9999      -9999      -9999      -9999      -9999
920.3436   17.49328   -9999      -9999      9.640299797058106 -9999      -9999      -9999      -9999      -9999
920.496    16.87804   -9999      -9999      9.020050048828123 -9999      -9999      -9999      -9999      -9999
920.6484   16.85216   -9999      -9999      8.067549705505371 -9999      -9999      -9999      -9999      -9999
920.8008   17.02463   -9999      -9999      7.293330192565918 -9999      -9999      -9999      -9999      -9999
920.9532   17.71181   -9999      -9999      6.372640132904053 -9999      -9999      -9999      -9999      -9999
921.1056   18.616     -9999      -9999      6.121819972991943 -9999      -9999      -9999      -9999      -9999
921.258    17.36493   -9999      -9999      6.807360172271729 -9999      -9999      -9999      -9999      -9999
921.4104   17.06421   -9999      -9999      7.753520011901856 -9999      -9999      -9999      -9999      -9999
921.5628   16.91022   -9999      -9999      8.14385986328125 -9999      -9999      -9999      -9999      -9999
921.7152   16.82972   -9999      -9999      8.418239593505859 -9999      -9999      -9999      -9999      -9999
```

1 of 2

```
1542.7452  17.07322   -9999      141.0596499999979 50.84585952758789 0.8196199999999113 -9999      -9999      0.8980699999998995 10.11721999999959
1542.8976  17.0725    -9999      141.2334999999997 51.39540100097656 0.850509999999953 -9999      -9999      0.9739999999999882 10.25874999999979
1543.05    17.24857   -9999      141.5783099999995 52.50205993652344 0.8665799999999758 -9999      -9999      0.9858099999999822 10.50375999999963
1543.2024  17.38271   -9999      142.27609  54.99422836303711 0.88834    -9999      -9999      0.97933    10.40947
1543.3548  17.40824   -9999      143.0828899999988 56.71345901489258 0.8941599999999912 -9999      -9999      0.9738000000000082 10.15400000000038
1543.5072  17.39879   -9999      144.76519  56.98733139038086 0.88689    -9999      -9999      0.97422    10.1634
1543.6596  17.35885   -9999      146.08838  56.6168212890625 0.87183    -9999      -9999      0.96872    10.16218
1543.812   17.3366    -9999      147.41939  57.53507995605469 0.83727    -9999      -9999      0.89541    9.916930000000001
1543.9644  17.33151   -9999      149.2517599999973 57.96939086914063 0.8078400000000432 -9999      -9999      0.8224600000001042 10.19077999999959
1544.1168  17.34412   -9999      150.7045299999979 59.00880813598633 0.7813300000000388 -9999      -9999      0.7884500000000497 10.33229999999979
1544.2692  17.73186   -9999      153.1944599999963 60.26184844970703 0.7683700000000192 -9999      -9999      0.7984699999999849 10.47380999999979
1544.4216  18.11727   -9999      154.7720099999976 61.01229095458984 0.7797399999999829 -9999      -9999      0.8550699999999126 11.21511999999889
1544.574   18.50516   -9999      155.5681699999988 61.94771957397461 0.7942999999999978 -9999      -9999      0.8973399999999354 11.94771999999891
1544.7264  19.02354   -9999      155.9584299999994 63.54471969604492 0.8011299999999898 -9999      -9999      0.9326299999999465 12.35384999999939
1544.8788  19.81139   -9999      155.94738  65.67936706542969 0.8096600000000001 -9999      -9999      0.96512    12.36303
1545.0312  21.95021   -9999      155.54116  66.60635375976563 0.81496    -9999      -9999      0.96241    12.76916
1545.1836  22.10902   -9999      155.7969599999996 65.92690277099609 0.820299999999992 -9999      -9999      0.936620000000038 12.77584999999999
1545.336   22.12184   -9999      155.78795  63.29977035522461 0.818980000000002 -9999      -9999      0.9087700000000408 12.91981999999979
1545.4884  22.12132   -9999      156.0776599999996 61.47354125976563 0.8092600000000144 -9999      -9999      0.8820900000000392 12.63860000000042
1545.6408  21.95027   -9999      156.2995399999997 60.02727890014648 0.7967100000000186 -9999      -9999      0.8591100000000339 12.39863000000036
1545.7932  20.36604   -9999      156.7642499999993 60.03647994995117 0.7874000000000138 -9999      -9999      0.8447100000000213 12.02115000000056
1545.9456  17.90893   -9999      157.0759099999995 61.18867874145508 0.7829600000000067 -9999      -9999      0.8246100000000296 11.76571000000038
1546.098   17.76194   -9999      156.43449  61.87815856933594 0.7691     -9999      -9999      0.80753    12.43192
1546.2504  17.71373   -9999      155.07762  61.35493850708008 0.7741400000000001 -9999      -9999      0.81175    13.18587
1546.4028  17.31215   -9999      153.1628500000029 60.79833984375 0.7744699999999996 -9999      -9999      0.8323799999999688 13.38093999999971
1546.5552  16.77301   -9999      151.2422600000029 59.351318359375 0.7843099999999852 -9999      -9999      0.8656299999999494 13.52240999999979
1546.7076  16.55391   -9999      149.1868200000031 57.84244918823242 0.7894499999999923 -9999      -9999      0.8953999999999548 13.41972000000015
1546.86    16.41308   -9999      147.5125200000025 57.24848175048828 0.8142299999999625 -9999      -9999      0.9234499999999576 13.40844000000002
1547.0124  16.76287   -9999      146.6892600000012 56.2706184387207 0.8427299999999567 -9999      -9999      0.9312599999999884 13.6797499999996
1547.1648  17.02546   -9999      145.7506900000014 54.82714080810547 0.8706299999999577 -9999      -9999      0.943299999999982 13.16217000000077
```

D: Zones of interest and llithology identification

D.1. Kofia-1 zones of interest

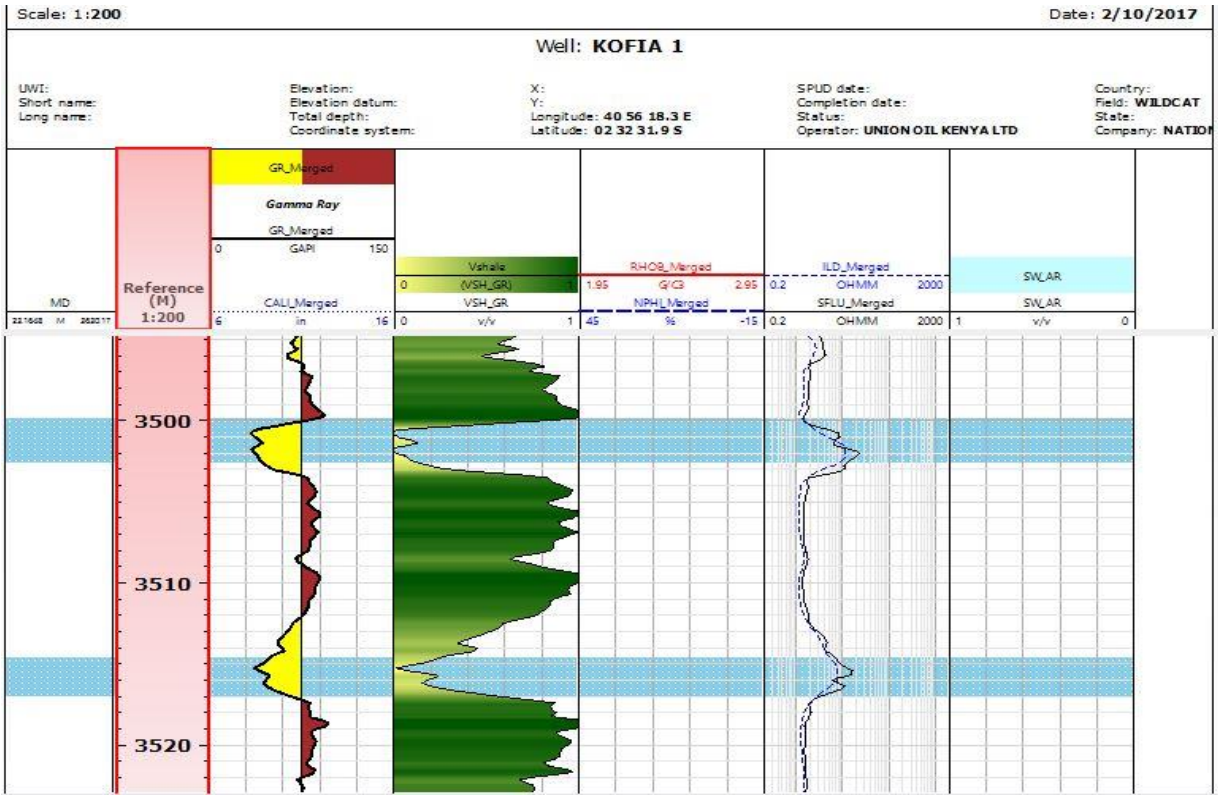

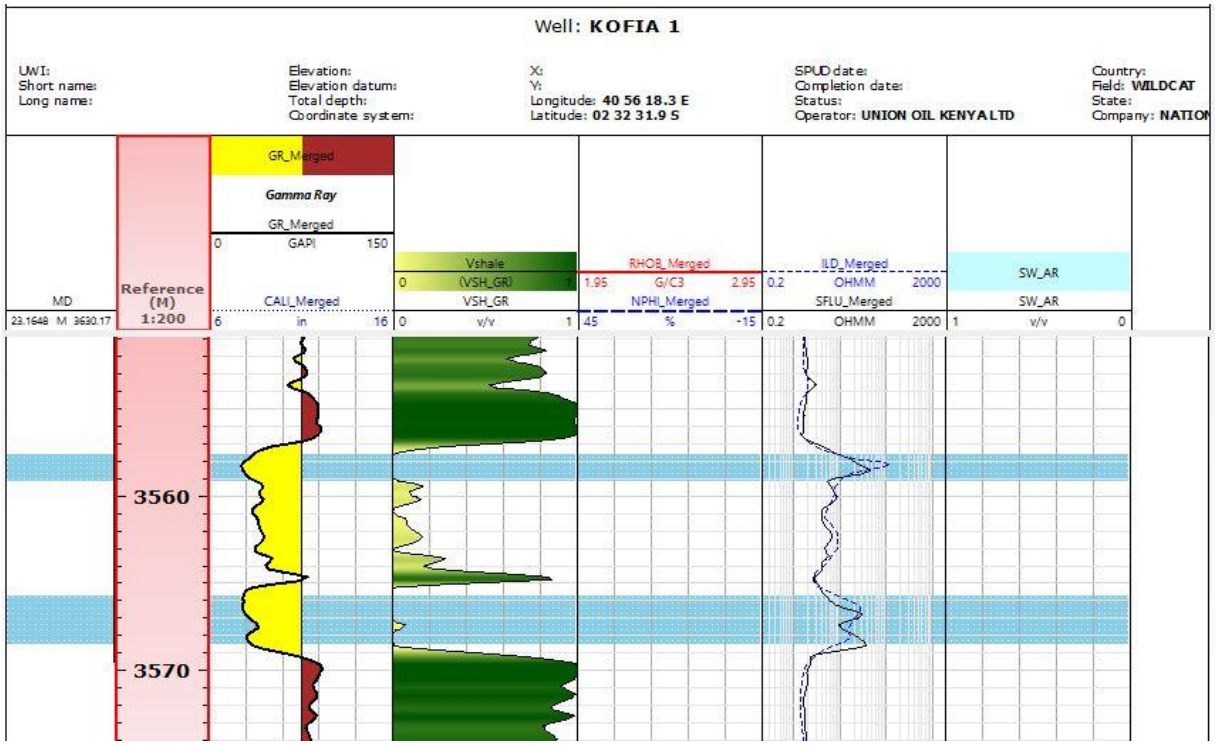

D.2. Simba-1 zones of interest

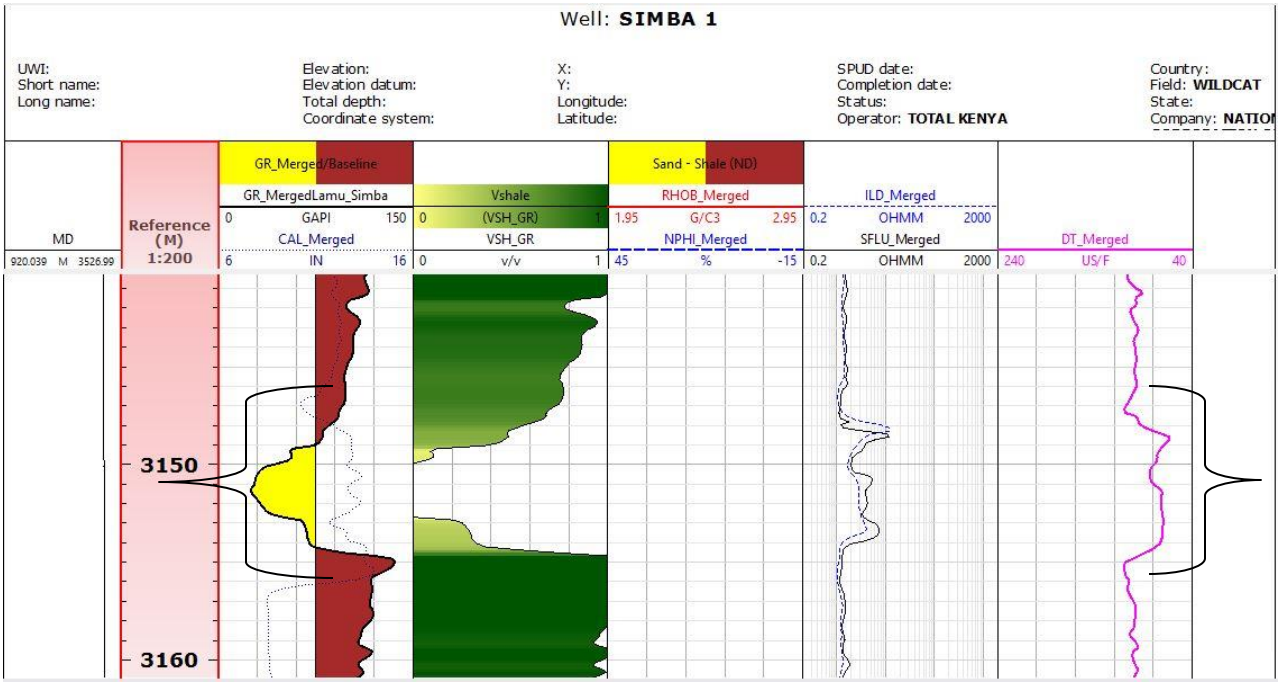

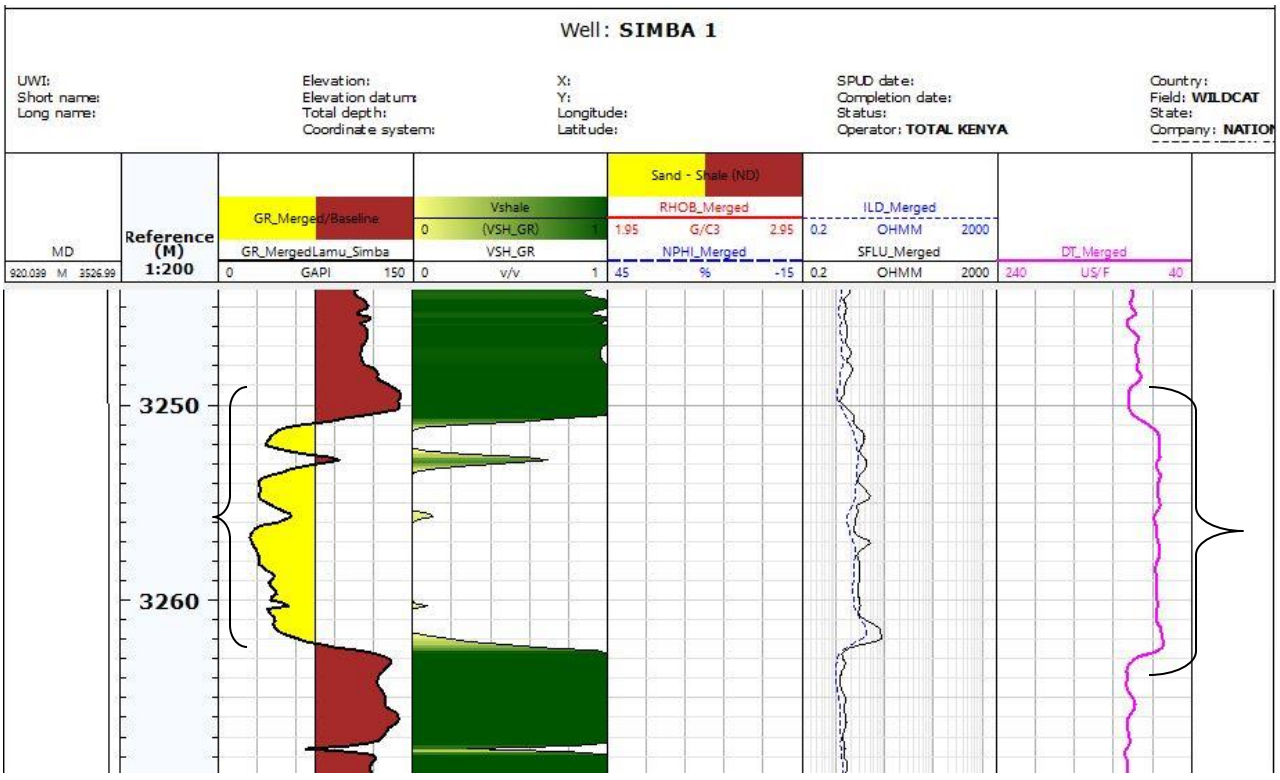

Some log details maybe lost in this interpretation, but the general lithology picture remains the same i.e. there could be minor intercalations of siltstone, dolomitic marls, and calcareous shale

D.3. Maridadi-1B zones of interest

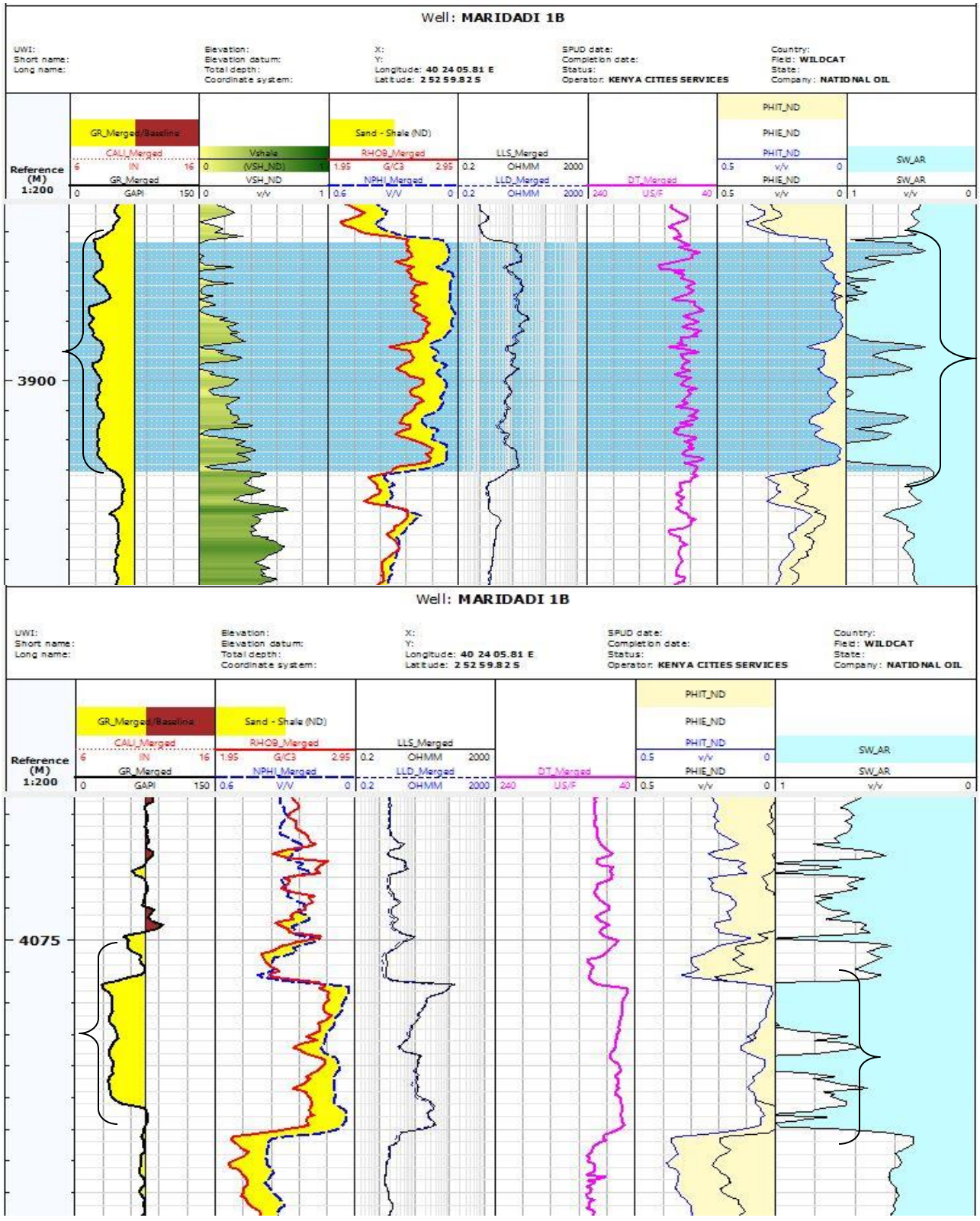

D.4. Simba-1 Lithology

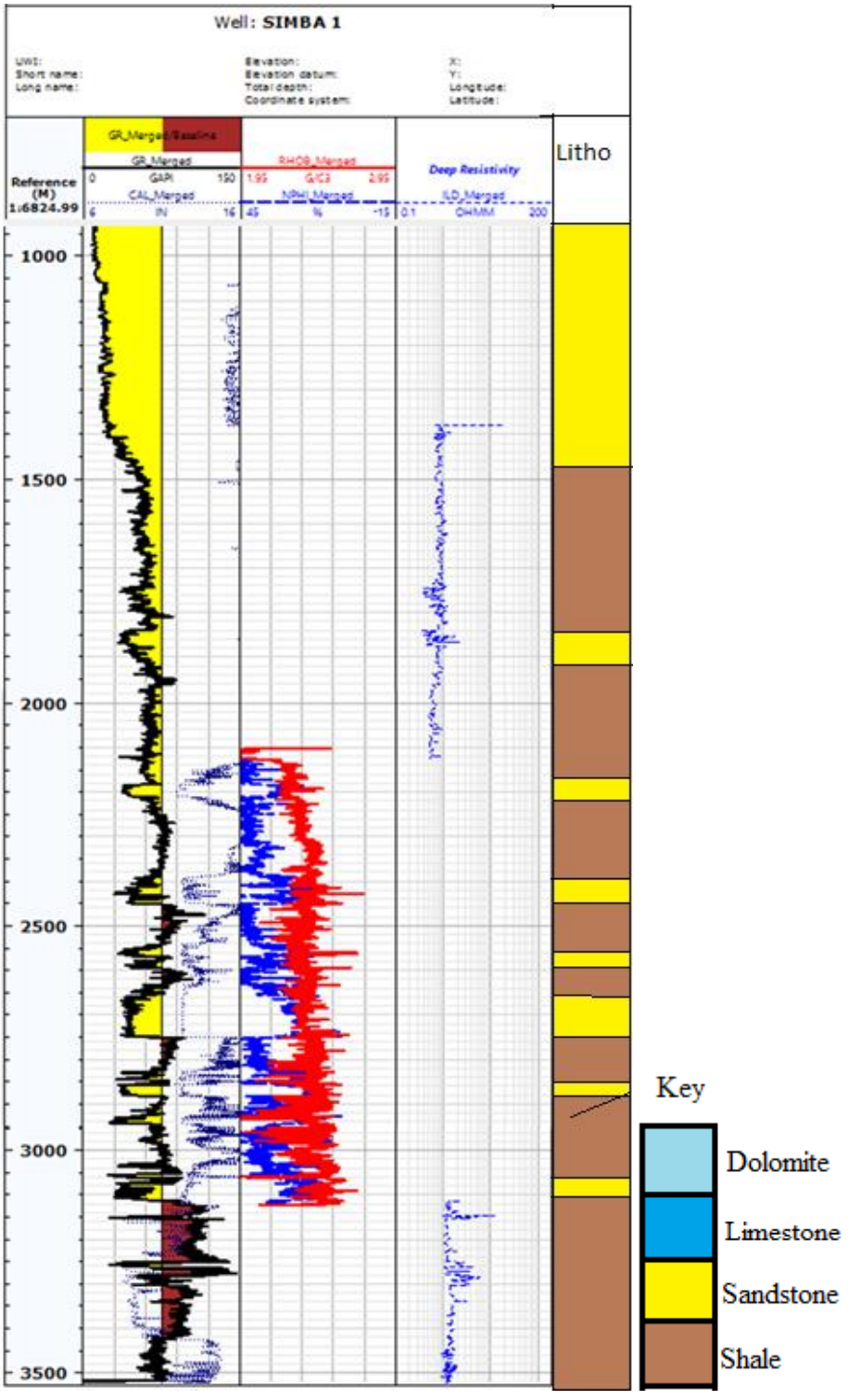

D.5. Kofia-1 Lithology

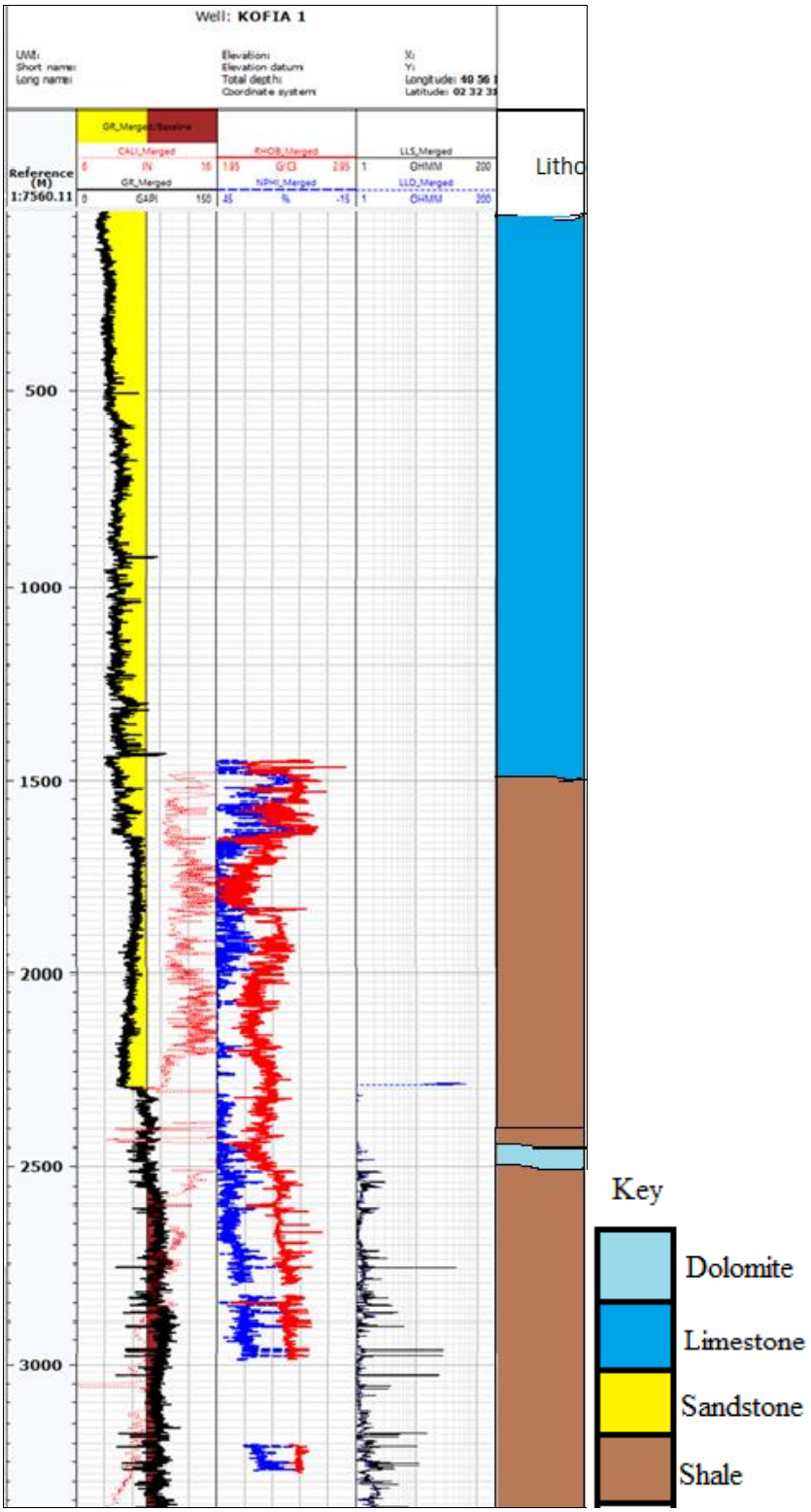

D.6. Maridadi-1B lithology

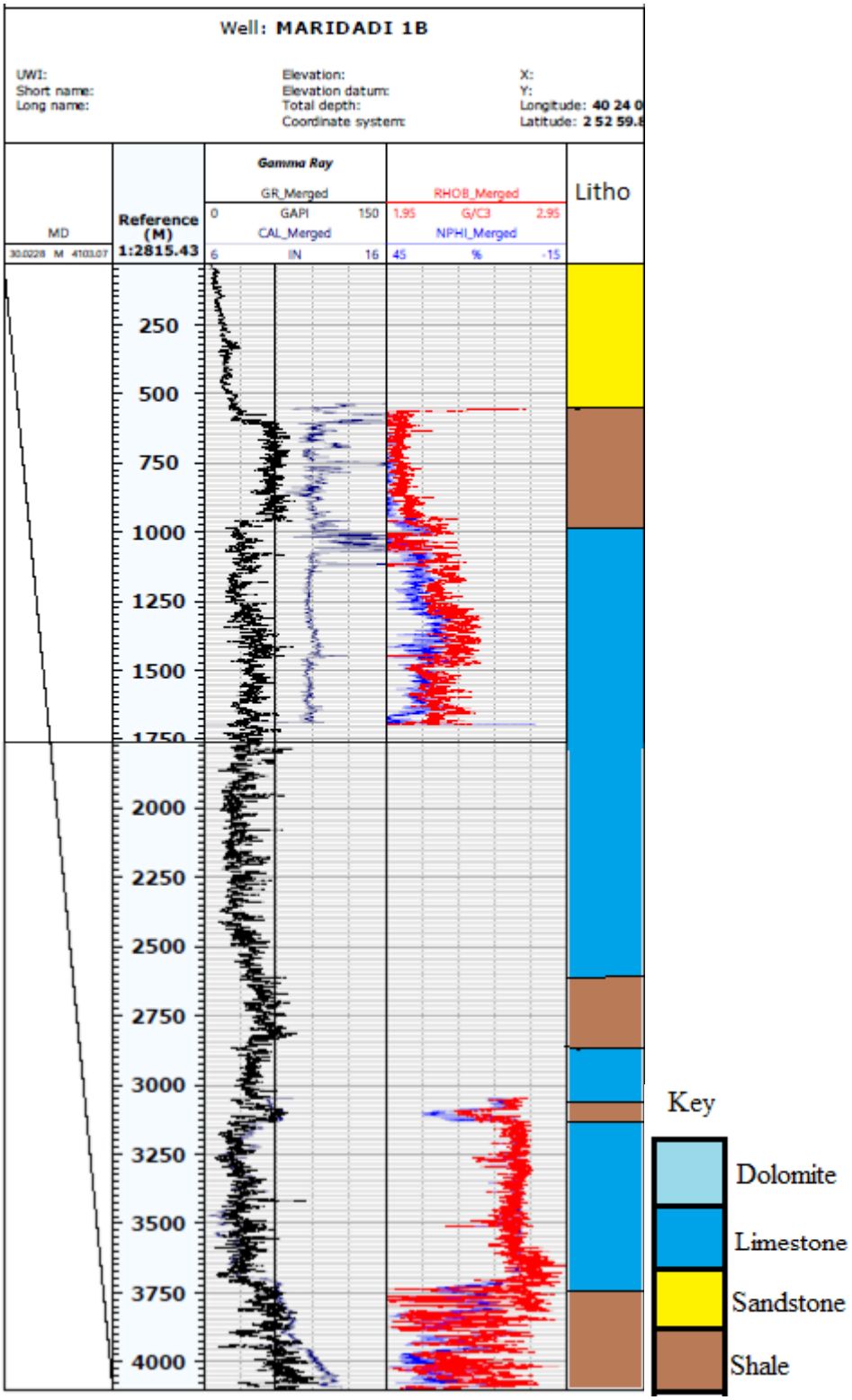

List of Definitions of Terminologies

API unit

The API (American Petroleum Institute) has established test pits for calibration of gamma and neutron. The API gamma unit is defined as 1/200 of the deflection between intervals of high and low radioactivity in the calibration pit. The API unit for the neutron is defined as 1/1,000 of the variance between electrical zero and the logged value opposite the Indiana limestone in the calibration pit with an average porosity of 19 percent.

Anomaly

Denotes to a deviation from consistency in a physical property.

Archie's Law

An empirical connection linking formation resistivity (Rt), porosity and formation water resistivity (R_w).

Bedrock

A broad term denoting the base rock below unconsolidated formation.

Bulk density

The mass of material per unit volume; in logging, it is the density, in gcc, of the rock with pore volume full of fluid.

Calibration

Definition of the log values that resemble to environmental units, for example bulk density or porosity; calibration is often conducted in pits or by appraisal with laboratory core analysis.

Caliper log

A continuous record of borehole diameter, usually made with a mechanical probe having from one to six arms.

Crossplot

A terminology applied in log analysis for a plot of one petrophysical parameter versus another, typically two different types of logs. Important in lithology identification.

Decay

In nuclear science, the process of breakup of an unstable radioisotope by the extemporaneous emission of particles or photons.

Density log

Also referred as gamma-gamma log; gamma photons from a radioactive source in the sonde are backscattered to a detector; the backscattering is related to the bulk density of the formation around the sonde.

Depth of investigation

Limit of signal penetration.

Effective porosity

The amount of interconnected pore space through which fluids can pass. Effective porosity is usually less than total porosity because some dead-end pores may be occupied by static fluid.

Flushed zone

The zone in the borehole wall behind the mudcake that is considered to have had all mobile native fluids flushed from it.

Formation

It denotes all geological material infiltrated by a drill hole without regard to its structure or lithology; applied in a stratigraphic literature, formation implies a named body of rock strata with common lithologic features.

Gamma log

Also termed as gamma-ray log or natural-gamma log; log of the natural radioactivity of the rocks penetrated by a drill hole.

Half-life

Radioactively, half-life is the time required for half of a given quantity of material to decay.

Invaded zone

The annular interval of material/rock around a drill hole where drilling fluid has substituted all or part of the formation interstitial fluids.

Isotopes

Atoms of the same element that have the same atomic number, but a different mass number; unstable isotopes are radioactive and decay to become stable isotopes.

Matrix

The solid framework of rock or mineral grains that surrounds the pore spaces.

Mud cake

The layer of mud particles that builds up on the wall of a rotary-drilled hole as mud filtrate is lost to the formation.

Neutron log

Neutrons from an isotopic source are recorded at one or several detectors after they travel through material in, and adjacent to, the wellbore. Log response primarily results from hydrogen content, but it can be related to saturated porosity and moisture content.

Nuclear log

Well logs using nuclear reactions either measuring response to radiation from sources in the probe or measuring natural radioactivity present in the rocks.

Sonde

Also called probe or tool; downhole well-logging instrument package.

Sonic log

Also called acoustic log; is a record of sound waves as they are transmitted through geological formation; the most common is a record of transit time.

Processing

Geophysically, to alter data so as to highlight certain aspects or correct for well-known influences, thereby enabling interpretation.

Radioactivity

Energy emitted as particles or rays during the decay of an unstable isotope to a stable isotope.

Receiver

The part of an acquisition system that senses the information signal.

Reservoir

Rocks or unconsolidated sediment that is capable of yielding a significant amount of hydrocarbons.

Saturation

The percentage of the pore space occupied by a fluid, usually oil or gas in hydrocarbon applications.

Self-potential (SP)

A geophysical method measuring the natural, static voltage existing between sets of points on the ground surface.

Sand base line

A line drawn through gamma logs deflections that represent sandstone; the same method can be used on SP log deflections to represent the average log response for shale (i.e. shale line).

Well log

A record that describes geologic formations and well test techniques applied in well construction. In this context it refers to a geophysical well log in which the physical properties of the formations are measured by geophysical tools, mainly nuclear logs.